

Synthesis, X-ray Structure Determination, and Comprehensive Photochemical Characterization of (Trifluoromethyl)diazirine-Containing TRPML1 Ligands

Kevin Schwickert, Michał Andrzejewski, Simon Grabowsky, and Tanja Schirmeister*



Cite This: *J. Org. Chem.* 2021, 86, 6169–6183



Read Online

ACCESS |



Metrics & More

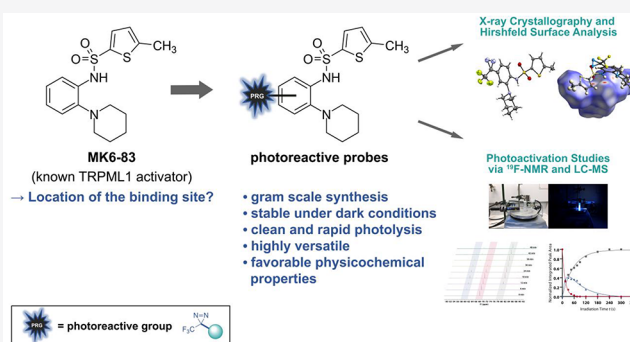


Article Recommendations



Supporting Information

ABSTRACT: Potential (trifluoromethyl)diazirine-based TRPML1 ion channel ligands were designed and synthesized, and their structures were determined by single-crystal X-ray diffraction analysis. Photoactivation studies via ^{19}F NMR spectroscopy and HPLC-MS analysis revealed distinct kinetical characteristics in selected solvents and favorable photochemical properties in an aqueous buffer. These photoactivatable TRPML1 activators represent useful and valuable tools for TRPML1 photoaffinity labeling combined with mass spectrometry.



INTRODUCTION

Mucopolipidosis type IV (MLIV) is an autosomal recessive lysosomal storage disease, which is clinically characterized by severe neurodegenerative defects, profound cognitive impairment, and eye abnormalities (e.g., corneal opacity, strabismus, and progressive retinopathy).^{1–4} These hallmark symptoms are often accompanied by other manifestations such as constitutive achlorhydria and iron deficiency anemia.^{5,6} MLIV patients also feature accumulated lysosomal inclusions containing different lipids and proteins that appear in almost all tissues, as demonstrated by electron microscopy.^{7–9} MLIV is caused by mutations in the *MCOLN1* gene, encoding mucolipin-1, a member of the transient receptor potential mucolipin (TRPML) cation channel subfamily.^{1,10,11} TRPML1 is a nonselective cation channel consisting of a six-transmembrane helix core and a large (~100 kDa) extracytosolic/luminal domain (ELD) that is exposed to the lysosomal lumen or the extracytosolic side of the cell.^{12–15} The main function of the TRPML1 channel is the Ca^{2+} ion transfer from the lysosome lumen to the cytoplasm, and its activity is influenced by different Ca^{2+} concentrations and pH values, therefore, playing a crucial role in vesicular transport, exocytosis, and autophagy.^{13,14,16} Currently, there are no specific treatment options for MLIV patients, particularly for those carrying mutations in the *MCOLN1* gene that result in complete TRPML1 absence in cells.^{3,17} Chen et al. identified a new small-molecule agonist of TRPML1 (MK6–83 (1), Figure 1), demonstrating its restoring effect on specific TRPML1 channel mutant isoforms and its ability to improve defects in endolysosomal trafficking as well as heavy metal ion homeostasis.¹⁷

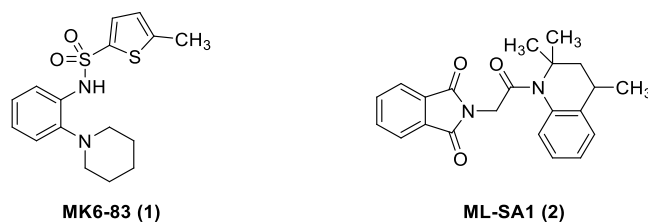


Figure 1. Structures of known TRPML channel agonists (see references for details).^{17–19}

These findings suggest that the TRPML1 activator MK6–83 may serve as a basis for a small-molecule treatment approach addressing a specific subgroup of MLIV patients.¹⁷ However, the exact location of the binding site of MK6–83 could not yet be determined, and currently, only cryo-EM structures of TRPML1 and TRPML3, respectively, bound with the nonselective and (structurally) different agonist (ML-SA1 (2), Figure 1)^{17,19} are available.^{20,21} It is not unambiguously clarified if MK6–83 addresses the same binding site within the channel and which key interactions are underlying to explain its different TRPML selectivity and activation profile compared to ML-SA1.²² For rational structure-based design and development of new drug

Received: December 22, 2020

Published: April 9, 2021



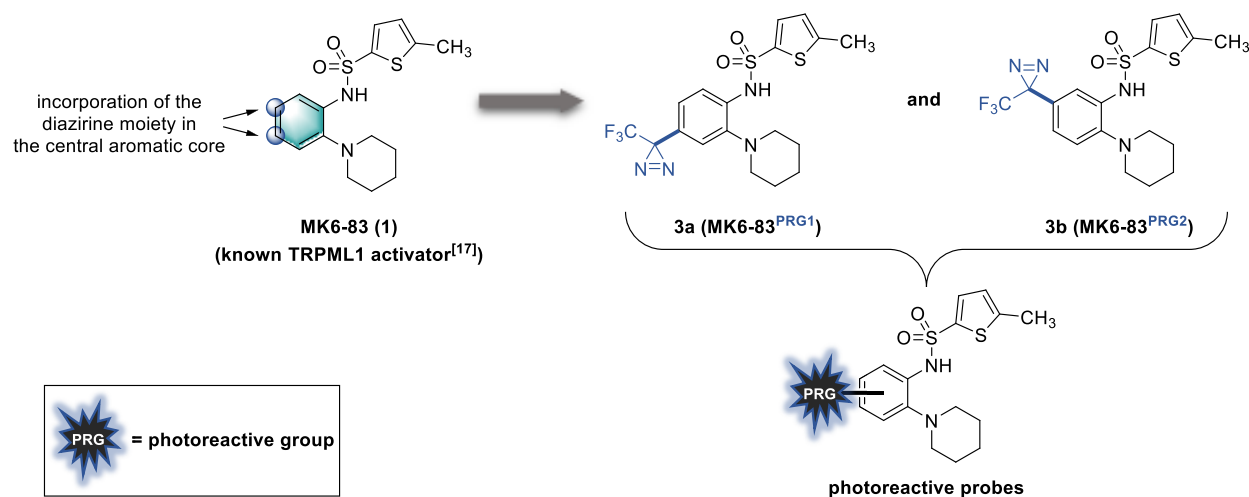
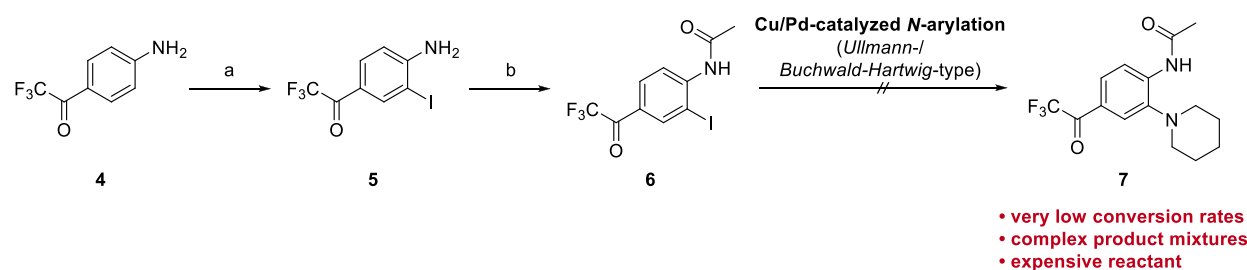


Figure 2. Design of new photoaffinity probes based on the known TRPML1 activator MK6–83.

Scheme 1. Initial Synthesis Route for the Introduction of the Piperidine Ring^a



^aReagents and conditions: (a) ICl, CaCO₃, MeOH/H₂O, rt, overnight, quant; (b) Ac₂O, 1,4-dioxane/H₂O, 0 °C → rt, overnight, 99%.

molecules, an in-depth understanding of ligand–target recognition and the interaction between the receptor protein and its small-molecule ligand is essential.^{23,24} In the past decades, photoaffinity labeling (PAL) has emerged as a very powerful tool in medicinal chemistry and chemical biology for studying ligand–target interactions and to provide additional information on the binding pocket and the amino acid residues involved in drug binding.^{25–30} This valuable technique exploits the intrinsic property of ligands featuring a photoreactive group (PRG) to produce a highly reactive species (e.g., a carbene), which, after the formation of a particular noncovalent ligand–receptor complex, covalently and irreversibly binds to proximate residues within the binding site during photolysis by irradiation with a specific wavelength of light.^{25,26,29,31} In this study, we focused on the synthesis as well as structural determination of novel (trifluoromethyl)diazirine-containing TRPML1 activators and extensively investigated their photochemical insertion reactivity in different solvents. These stable and useful photoactivatable analogues of MK6–83 may allow the identification of the binding site within the TRPML1 channel and thus make a relevant contribution to the elucidation of the molecular mechanisms involved in the specific ligand–protein interaction between the TRPML1 activator and its target ion channel.

RESULTS AND DISCUSSION

Design of the Photoaffinity Probes (PAPs). In designing new photoaffinity probes (PAPs) for cross-linking experiments with TRPML1 channels, we used the known TRPML1 activator MK6–83 as the parent molecule.¹⁷ We started our design with general considerations and requirements regarding the proper-

ties for the PAPs: (i) the incorporated photoreactive group (PRG) should be as small as possible, minimizing the risk of significantly altering the biological activity of the parent molecule; (ii) the modified activator should exhibit relative chemical stability in the dark at room temperature; (iii) cross-linking should be specific and possible at higher wavelengths (~360 nm), reducing the risk of damage to targeted proteins. Based on this discussion, the frequently used azido group was not considered since the shorter wavelengths required for excitation ($\lambda < 300$ nm) can cause significant damage to biological molecules, and the nitrene intermediates and rearranged ketenimines formed during photolysis can result in decreased photoaffinity yields and nonspecific labeling.^{31–33} Consequently, we envisioned that the introduction of a (trifluoromethyl)diazirine group would meet our criteria as it represents a relatively small PRG among all commonly used photophores. This keeps the structural changes of the parent molecule to a minimum, and its physicochemical properties are not substantially altered (contrary to, e.g., benzophenones).^{31,32} Furthermore, diazirines generate highly reactive carbenes upon photoactivation with longwave (~360 nm) UV light, and their selective cross-linking property reduces the risk of nonspecific binding due to the short lifetime of the reactive intermediate.^{28,31,32,34} Their relative chemical stability (e.g., under acidic and basic conditions, toward nucleophiles and electrophiles) enables easy handling and performance of demanding synthetic transformations.^{26,32,35}

We decided to use the pre-existing phenyl ring of the parent ligand MK6–83 as the most suitable substitution site for PRGs (Figure 2) since structural modifications such as chlorine at the 5'-position of the aromatic core only slightly reduced efficacy on

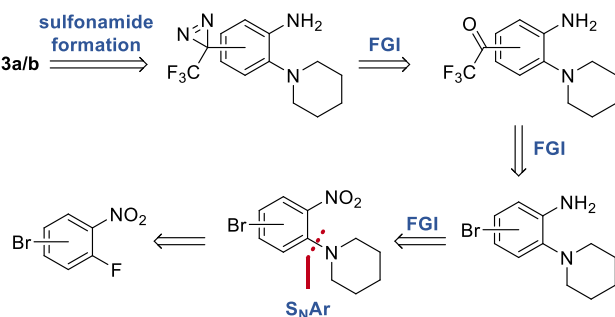
TRPML1 activation whereas larger substituents at the thiophene ring and other residues than piperidine affected the activity significantly.¹⁷ In addition, the central orientation of the reactive group within the whole molecule should facilitate cross-linking with a residue of the potential binding site. We further assumed that generating two constitution isomers of the diazirine-containing PAPs, in which the PRG is attached at different positions along the aromatic core, would provide an opportunity to perform binding site mapping and thus to achieve an increased topological resolution of the cavity.^{31,35}

■ SYNTHESIS

Our initial approach to the target diazirines involved the introduction of the piperidine residue in iodoaniline **6** via a copper- or palladium-catalyzed *N*-arylation reaction.^{36–38} The latter compound was synthesized in a sequence including selective *ortho*-monoiodination with iodine monochloride³⁹ and acetylation using acetic anhydride and catalytic amounts of sulfuric acid (Scheme 1).⁴⁰

Unfortunately, multiple attempts to realize the amination reaction of **6** were not satisfactory, as low conversion rates associated with the formation of complex product mixtures were observed in each case. Further optimization of this reaction was not undertaken because **4** represented an expensive reactant, and a different synthesis route was developed simultaneously that was much more attractive from an economic point of view and in terms of scalability. Retrosynthetic analysis in this alternative approach identified 4- and 5-bromo-2-fluoro-1-nitrobenzenes as inexpensive and commercially readily available starting materials, thus bypassing transition metal-catalyzed *N*-arylation in favor of nucleophilic aromatic substitution to introduce the required piperidine ring (Scheme 2).

Scheme 2. Retrosynthetic Analysis for the Synthesis of Diazirine 3a^a



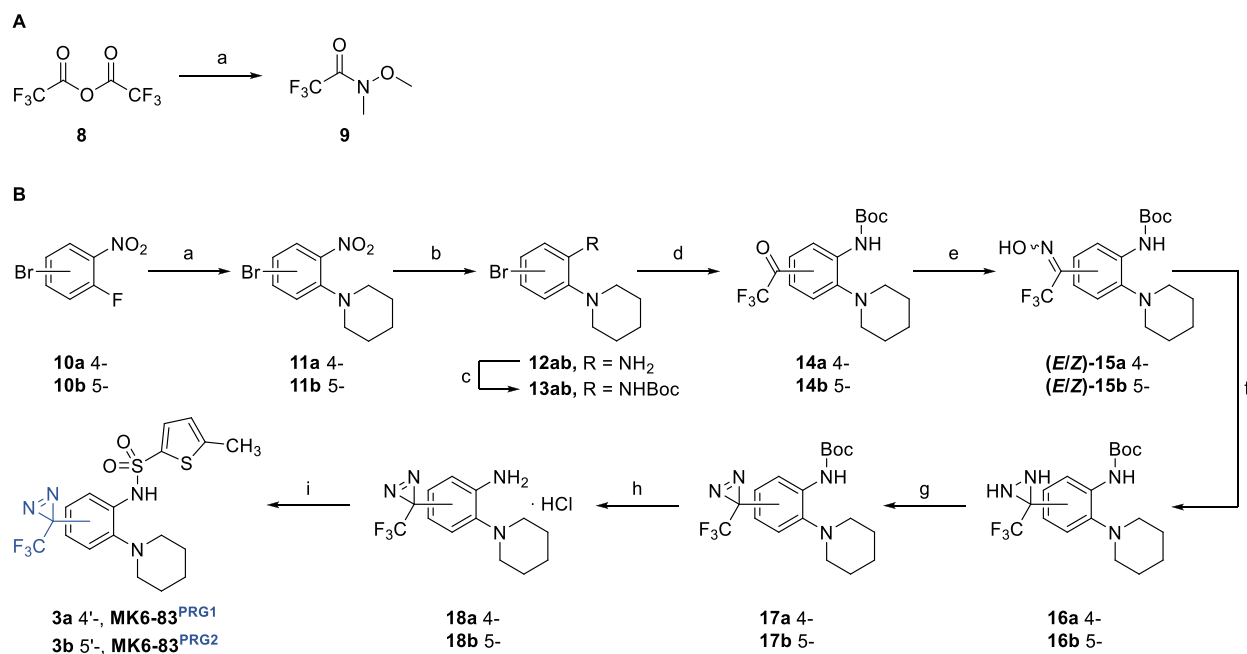
^aFGI: Functional group interconversion.

Therefore, the final multistep syntheses of the new photoaffinity probes MK6–83^{PRG1} (**3a**) and MK6–83^{PRG2} (**3b**) started from commercially available 4- or 5-bromo-2-fluoro-1-nitrobenzenes, in which a piperidine ring was introduced by the application of a nucleophilic aromatic substitution using Cs₂CO₃ as a base to give **11a** and **11b** in high yields (Scheme 3B).⁴¹

The nitro derivatives **11a** and **11b** were then reduced to provide the corresponding anilines **12a** and **12b** using SnCl₂·2 H₂O.⁴¹ Boc-protection of **12a** was accomplished with Boc₂O in the presence of the Lewis acid Zn(ClO₄)₂·6 H₂O as the catalyst.⁴² Since this procedure was not suitable for the protection of **12b** due to longer reaction times and side reactions such as biscarbamylation, an alternative method using

NaHMDS⁴³ as a strong base for the introduction of the Boc group was applied to obtain **13b**. Our initial synthetic approach by this route involved the use of an acetyl protecting group, which was introduced in one step in a reduction and acetylation reaction starting from the nitro derivative **11a** using zinc dust in a mixture of glacial acid and acetic anhydride. Unfortunately, the harsh acid or basic conditions required for its deprotection led to the decomposition of the diazirinyl ring (data not shown). Therefore, we selected the Boc group as a comparatively more labile protective group, which proved to be well suited for the established synthesis route since no ring opening was observed during removal. For the preparation of the key intermediate (trifluoromethyl)ketones **14a** and **14b**, the bromo derivatives **13a** and **13b** were subjected to a trifluoroacetylation reaction, which was achieved via NH-deprotonation with potassium hydride⁴⁴ at 0 °C, followed by a subsequent halogen-metal exchange with ^tBuLi⁴⁵ at –78 °C and treatment of the *in situ* formed organolithium compound with 2,2,2-trifluoro-*N*-methoxy-*N*-methylacetamide (**9**, prepared from trifluoroacetic anhydride and *N,O*-dimethylhydroxylamine hydrochloride^{46,47} (Scheme 3A)). The deprotonation step in the trifluoroacetylation sequence was crucial since it turned out that the halogen-metal exchange competed with NH-abstraction, leading to a significant reduction in yield due to the formation of the corresponding dehalogenated side-product. The trifluoroacetylated compounds **14a** and **14b** were then converted to oximes **15a** and **15b** with hydroxylamine hydrochloride in pyridine/ethanol under reflux, which were isolated as a mixture of *E/Z*-diastereomers (88% and 96% yields, respectively) and subsequently tosylated with tosyl chloride under basic conditions at 0 °C. The obtained *O*-tosyl oximes were immediately used for the next step without further purification because of their instability on silica and warming during evaporation. The construction of the (trifluoromethyl)-diazirine moiety on the aromatic core was realized by reaction of the tosylated oximes with liquid ammonia at –78 °C to give diaziridines **16a** and **16b** in 99% and 86% yields, respectively, which were then oxidized with iodine/NEt₃ in CH₂Cl₂ to provide the photoreactive diazirines **17a** and **17b**. Deprotection of the amino group using HCl (4.0 M in 1,4-dioxane) went smoothly without affecting the diazirine ring, and the hydrochlorides **18a** and **18b** were isolated in quantitative yields. Formation of the sulfonamide with 5-methylthiophene-2-sulfonyl chloride in pyridine at 0 °C completed the synthesis, and the final photoaffinity probes were obtained in good yields (63% and 72%, respectively) and high purity (≥99%) as confirmed by HPLC-MS analysis (Figures S1 and S2). The synthesized compounds retain their stability even after several months of storage in the dark at –21 °C under an argon atmosphere. No decomposition of **3a** and **3b** could be observed, providing both, the 4'- and 5'-(trifluoromethyl)diazirine-substituted analogue, as stable and easy-to-handle reagents for photoaffinity labeling purposes.

With the HPLC-MS analysis, we also investigated the fragmentation pattern of the synthesized diazirines to evaluate their stability under electrospray ionization (ESI) MS/MS conditions and to identify potential fragments in mass spectrometry experiments that might occur after the photoaffinity labeling procedure with proteins. For both compounds, a high abundance of the parent ion [M + H]⁺ (*m/z* = 445.1) was observed with only a minor amount of a fragment ion (*m/z* = 417) resulting from the loss of molecular nitrogen ($\Delta m/z = 28$) (Figures S5 and S6, Schemes S1 and S2). Under collision-

Scheme 3. Final Synthesis of the (Trifluoromethyl)diazirine-substituted TRPML1 Activators^a

^aReagents and conditions: [A] (a) *N,O*-dimethylhydroxylamine hydrochloride, py, CH₂Cl₂, 0 °C, 2 h, 64%; [B] (a) piperidine, Cs₂CO₃, DMF, rt, overnight, 99%; (b) SnCl₂·2 H₂O, EtOAc, rt, 1 h—overnight, 93–96%; (c) **12a**, R = NH₂; **12b** Boc₂O, NaHMDS (1.9 M in THF), THF, rt, overnight, 60%; (d) (1) KH (30% suspension in mineral oil), 0 °C, 1 h; (2) ^tBuLi (1.6 M in pentane), 5, –78 °C, 6 h, 66–77%; (e) NH₂OH·HCl, py/EtOH, 80 °C, 4–5 h, 88–96%; (f) (1) TsCl, Et₃N, acetone; 0 °C, 3 h; (2) NH₃ (1), MTBE, –78 °C → rt, overnight, 86–99%; (g) I₂, Et₃N, CH₂Cl₂, 0 °C → rt, 2 h, 82–95%; (h) HCl (4.0 M in 1,4-dioxane), rt, 1–2 h, quant; (i) 5-methylthiophene-2-sulfonyl chloride, py, 0 °C → rt, overnight, 63–72%.

induced dissociation (CID) conditions (MS/MS), the precursor ion was completely converted to the above-mentioned fragment ion, which in the case of constitution isomer **3a** was accompanied by trace amounts of another product ion (4%, $m/z = 255.1$) as a consequence of additional loss of the 5-methylthiophene-2-sulfonyl moiety or cleavage of the entire sulfonamide residue without extrusion of nitrogen (3%, $m/z = 268.1$). Fragmentation of diazirine **3b**, on the other hand, resulted in a concurrent appearance of a different product ion with approximately 60% abundance ($m/z = 240.0$), in which the whole sulfonamide fragment was presumably dissociated in addition to the loss of nitrogen. The high abundance of the precursor ions in the LC-MS mode, as well as the occurrence of defined product ions under application of moderate collision energy, indicates that the (trifluoromethyl)diazirines **3a** and **3b**, respectively, exhibit outstanding structural integrity and stability under ESI-MS conditions, which facilitates the identification of labeled protein residues or amino acids after photoaffinity labeling.

X-RAY STRUCTURE DETERMINATION

Single-crystal X-ray diffraction data of **3a** and **3b** were collected at 100 K on a Rigaku SuperNova diffractometer with MoK α radiation using an Eos CCD detector. The structures were solved and refined inside Olex2⁴⁸ with the SHELXT⁴⁹ and the SHELXL⁵⁰ software, respectively (Figure 3 and Figure S4). Both compounds crystallize in the monoclinic *P*2₁/*c* space group. Selected crystallographic data for **3a** and **3b** are listed in Table 1. Full experimental and crystallographic data are in Table S1.

In the context of quantum-crystallographic electron-density research, the inter- and intramolecular bonding of biologically active vinyl sulfone groups has been studied in detail.^{51,52}

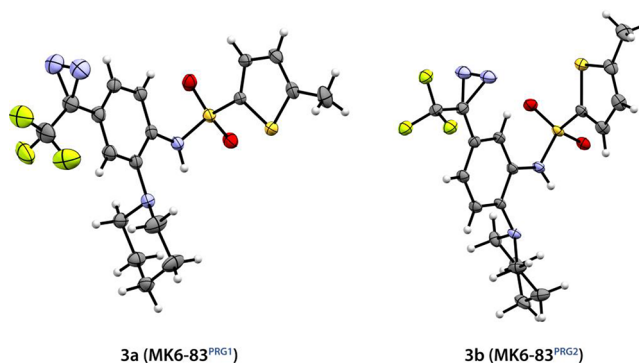


Figure 3. Crystal structures (ORTEP) of the studied compounds **3a** and **3b**. Thermal ellipsoids are displayed with 50% probability.

Table 1. Selected Crystallographic Data for **3a** and **3b**

parameter	3a (MK6–83 ^{PRG1})	3b (MK6–83 ^{PRG2})
a (Å)	14.8659(2)	15.34810(10)
b (Å)	7.68040(10)	8.43370(10)
c (Å)	17.72280(10)	16.1087(2)
β (°)	101.6910(10)	111.7130(10)
volume (Å ³)	1981.54(4)	1937.19(4)
Z	4	4
ρ_{calc} (g cm ^{–3})	1.490	1.524
R_{int}	0.0362	0.0543
R_1	0.0457	0.0527
wR_2	0.1372	0.1544

Moreover, the motif of an aziridine three-membered ring in protease inhibitor model compounds has been scrutinized by experimental quantum crystallography.^{53,54} Therefore, we had a

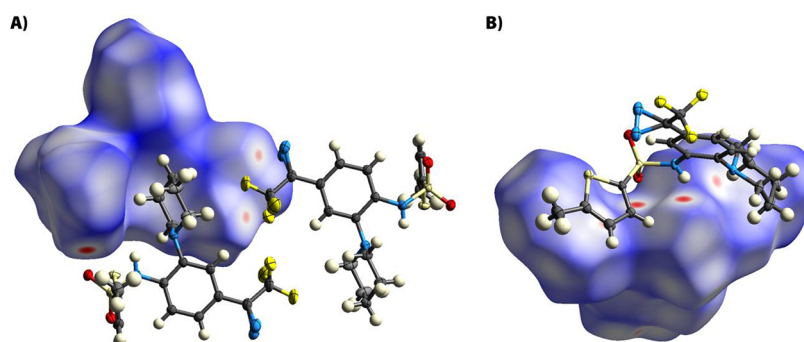
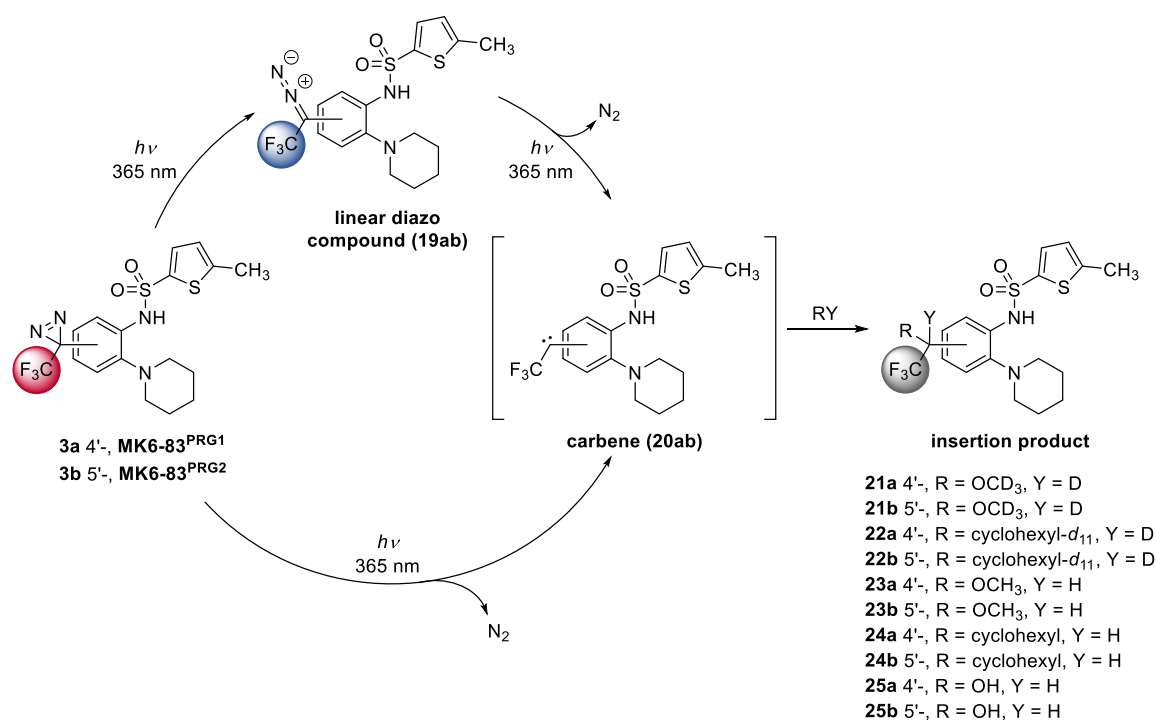


Figure 4. Hirshfeld surfaces of (A) **3a** and (B) **3b** color coded with the property d_{norm} . The color range is -0.1773 (red) to 0 (white) to 1.4995 (blue). Red dots represent short atom–atom contacts, and the symmetry-generated interaction partners outside the Hirshfeld surfaces are given. Displacement ellipsoids and spheres are given at a 50% probability level. The pictures were generated with the software CrystalExplorer (see reference for details).⁵⁹

Scheme 4. Photoactivation Reaction of Diazirines **3a** and **3b** in Different Solvents



closer look at the three-membered diazirine ring motif here in comparison to the aziridine motif, although disorder and reduced resolution of the data prevented an electron-density analysis (Figure S4). The N–N bond is quite short with 1.228(3)/1.218(2) Å in **3a/b**, and the two C–N bonds are long, being just below 1.50 Å. In the aziridine three-membered ring, the C–N bonds are significantly shorter at 1.45 Å.^{53,54} The C–N–N angles are between 65–66° and the N–C–N angle below 49° in both compounds **3a/b** leading to an acute triangle, whereas, in aziridine, all three angles are around 60°. These geometric details point toward an asymmetric distribution of electron density in the three-membered ring, an accumulation of electron density in the N–N bond, and hence a different reactivity than aziridine-containing biologically active compounds.

Since it is known that geometrical and electron-density features of biologically active compounds in small-molecule crystal structure packings can resemble those in biological ensembles,^{55,56} we employed Hirshfeld Surface Analysis⁵⁷ here

to get an overall picture of the intermolecular interactions that dominate the crystal packing in **3a** and **3b**, respectively (Figure 4; red dots highlight close intermolecular interactions). In **3a**, there is only a C–H⋯O hydrogen bond involving the sulfonyl group, but the N–H group does not act as a hydrogen bonding donor (Figure 4 (A)). Instead, there is a remarkably short inverse diaziridine–CF₃ intermolecular contact, basically a N⋯F interaction between two electron-rich atoms, which deserves further study in the context of recent discussions around halogen and pnictogen bonding.⁵⁸

In contrast, the crystal packing in **3b** is dominated by the more usual inverse N–H⋯O_{sulfonyl} bonding motif one might expect with a N–H hydrogen bonding donor group present in the structure. Obviously, this N–H group is more accessible for intermolecular interactions because of the *meta*- instead of *para*-substitution of the phenyl ring in **3b**. The diaziridine–CF₃ contact is present in **3b**, too, but less pronounced, and there is no C–H⋯O hydrogen bond either. In summary, the difference in substitution leads to significantly different crystal packings in

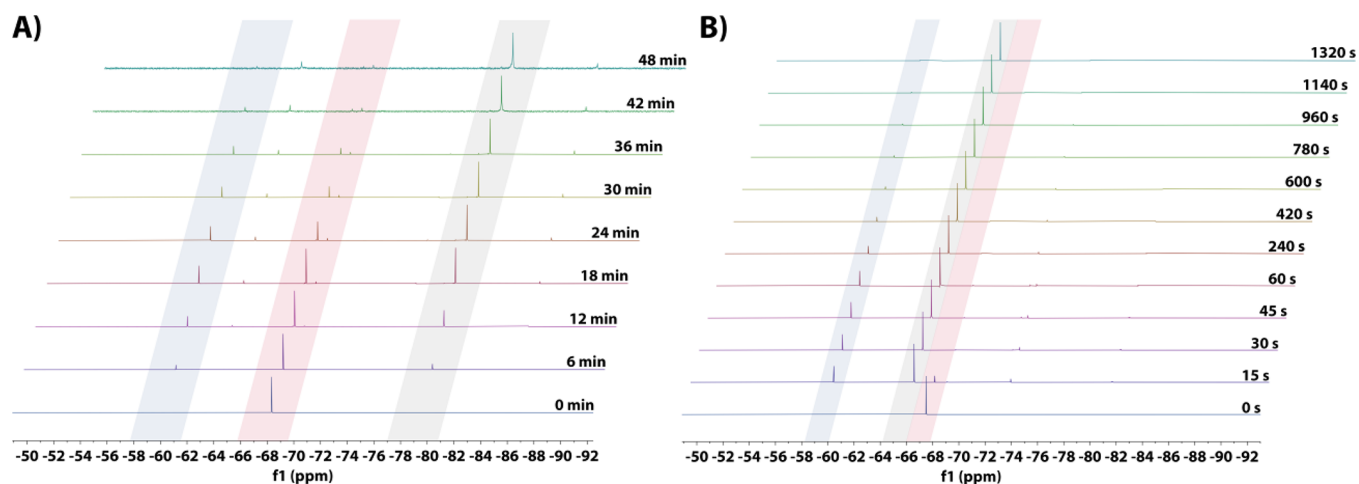


Figure 5. ^{19}F NMR spectra of a 5 mM solution of **3a** in methanol- d_4 (A) and cyclohexane- d_{12} (B) upon irradiation with UV light ($\lambda = 365$ nm) recorded at different irradiation intervals. Spectra are shifted for better visualization, and signals of the diazirine, linear diazo isomer, and the corresponding insertion product are highlighted in red, blue, and gray, respectively (see Scheme 4). For ^{19}F NMR spectra of the photoinduced decay of the constitution isomer **3b**, see Figure S7.

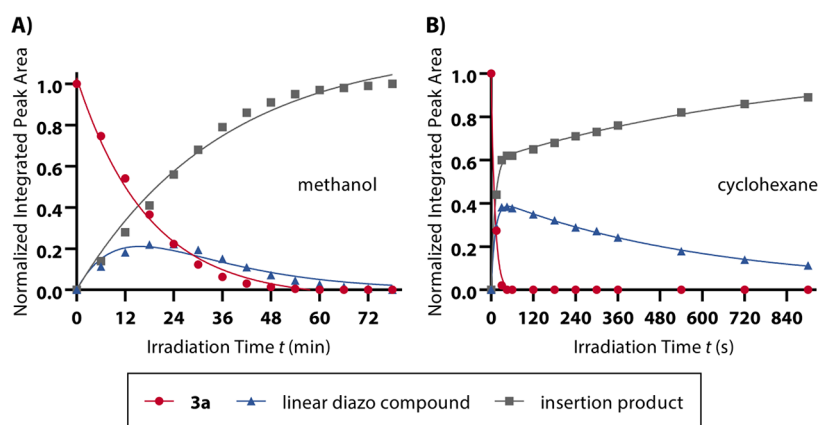


Figure 6. Photoinduced decay of diazirine **3a** ($c = 2$ mM; $\lambda = 365$ nm) in methanol (A) and cyclohexane (B) investigated via HPLC (C_{18}). Aliquots were collected and analyzed at different time intervals of UV activation. The resulting peak areas (UV detection at $\lambda = 254$ nm) of the diazirine (red, circles), linear diazo compound (blue, triangles), and the insertion product (gray, squares) in the chromatograms were integrated and plotted against the irradiation time after normalization. Diazirine turnover and product formation can be fitted by first-order exponential functions, while the evolution and subsequent decay of the linear diazo isomer can be expressed by a biexponential trend line.

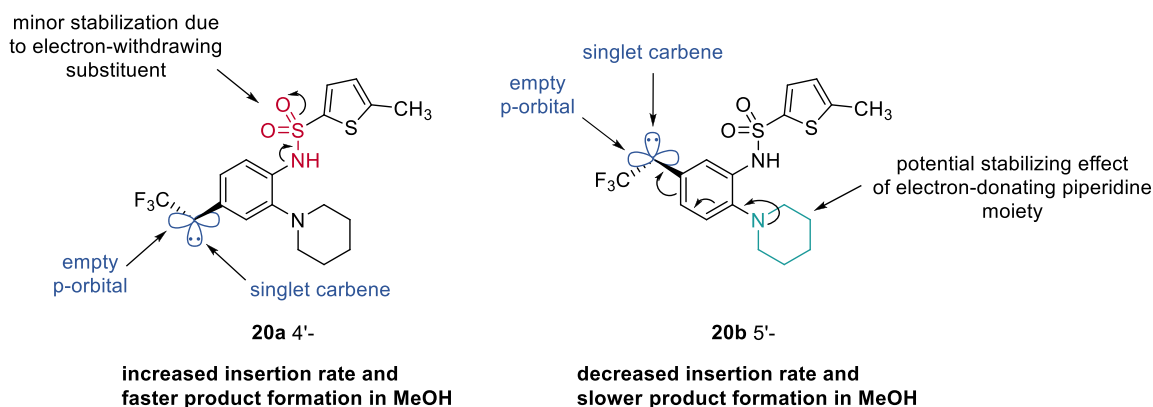


Figure 7. Potentially different influence of the substitution pattern on the carbene stability in **20a** and **20b** explaining the heterogeneous reactivity and product formation times of both constitution isomers.

both compounds, which might have consequences on their

activities.

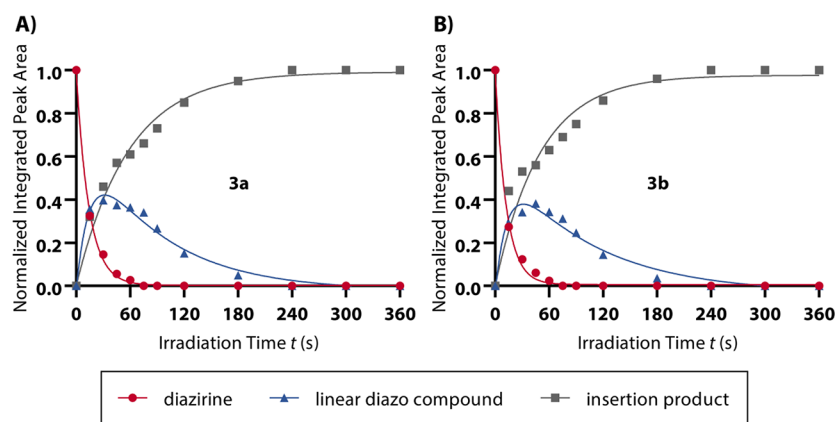


Figure 8. Investigation of the photoinduced decay of diazirines **3a** (A) and **3b** (B) ($c = 50 \mu\text{M}$; $\lambda = 365 \text{ nm}$) in aqueous buffer (50 mM TRIS, 150 mM NaCl, 2 mM CaCl_2 , 5 mM KCl, 5 mM MgCl_2 , 4 mM EDTA, and 250 mM sucrose) via reversed-phase HPLC. Aliquots were collected and analyzed at different time intervals of UV activation. The resulting peak areas (UV detection at $\lambda = 254 \text{ nm}$) of the diazirine (red, circles), linear diazo compound (blue, triangles), and the insertion product (gray, squares) in the chromatograms were integrated and plotted against the irradiation time after normalization. Diazirine turnover as well as the product formation can be fitted by first-order exponential functions, while the evolution and subsequent decay of the linear diazo isomer can be expressed by a biexponential trend line.

KINETICAL CHARACTERIZATION OF THE PHOTOCHEMICAL REACTION OF **3a** AND **3b**

Next, we investigated the kinetical photoactivation behavior of the new TRPML photoaffinity probes in different media.^{34,60–62} Solutions of **3a** and **3b** in the appropriate (deuterated) solvent (methanol($-d_4$), cyclohexane($-d_{12}$), and aqueous buffer as carbene scavengers) were exposed to UV light ($\lambda = 365 \text{ nm}$) delivered by a high-power UV LED (Opsytec Dr. Gröbel GmbH, Germany) for different irradiation intervals, ^1H and ^{19}F NMR, respectively, as well as HPLC-MS spectra were recorded to monitor the course of the photoinduced diazirine decay (see Scheme 4, Figure 5, Figure 6, Figure 7, Figure 8, Figure S7, and Figure S8). First, the photolysis reactions were performed in deuterated methanol and cyclohexane ($c = 5 \text{ mM}$), respectively, and the signal changes of the fluorine signals (CF_3 group) were followed by ^{19}F NMR spectroscopy at various time intervals. Upon irradiation with UV light, diazirines **3a** and **3b** ($\delta = -68 \text{ ppm}$) completely underwent photolysis in methanol within 48 min (**3a**) and 78 min (**3b**) to form either the insertion products **21a/b** ($\delta = -79 \text{ ppm}$) or the linear diazo isomers **19a/b** ($\delta = -60 \text{ ppm}$) (Figure 5 and Figure S7) as a result of photoisomerization which is in competition with the appearance of the singlet carbene.

The observed photolytic characteristics and chemical shifts are in accordance with studies and spectral data reported for other aromatic (trifluoromethyl)diazirines.^{34,60,62} The linear diazo compound was converted to the methyl ether on further UV light exposure, as indicated by the subsequent decrease of the corresponding ^{19}F NMR signal under continued irradiation. Remarkably, the photoactivation kinetics of **3a** and **3b** in cyclohexane- d_{12} strikingly differed from the experiments in methanolic solution since complete decay of the diazirines was already observed after 30 s, while the lifetime of the linear diazo compound relative to the diazirines proved to be significantly longer (full conversion after 960 and 1320 s for **3a** and **3b**, respectively). This deviation can be explained by different abilities of the solvents to exert a stabilizing effect on the intermediate formed singlet carbene. In several studies, it could be shown that polar solvents like methanol preferably stabilize the singlet carbene by the interaction of the empty p orbital with nonbonding electrons of the solvent.^{63,64} Nevertheless, our

results proved that diazirines **3a** and **3b** even readily undergo rapid photolysis in a nonpolar environment suggesting that the insertion reaction can also take place with hydrophobic amino acid residues (e.g., leucine or valine) within the binding site. For a more quantitative description and physicochemical characterization, the photochemical reactions of (trifluoromethyl)diazirines **3a** and **3b** in methanol and cyclohexane ($c = 2 \text{ mM}$) were additionally followed by HPLC-MS analysis. Since photoaffinity labeling experiments are commonly accomplished in aqueous media, we also investigated the photochemical properties of these compounds in an aqueous buffer solution ($c = 50 \mu\text{M}$), e.g., to define the reaction conditions required for high-yield cross-linking of biological samples. Aliquots from the irradiation experiment were taken after fixed periods of time and subjected to LC-MS analysis, and the resulting peak areas (UV detection at $\lambda = 254 \text{ nm}$) of the diazirines **3a** and **3b**, linear diazo compounds **19a/b**, and the insertion products **23ab–25ab** were integrated. As expected, the obtained results agreed well with the observations of the ^{19}F NMR spectroscopy data (vide supra) since similar irradiation times were required for the complete photolysis of the starting material and the normalized integrated peak areas confirmed the recorded signal intensities in the ^{19}F NMR experimental setup (Figure 6 and Figure S8).

Parallel controls proved that the diazirines remained unaffected in the absence of a light source (data not shown). In all solvents, approximately first-order kinetics were obtained for the photolytic diazirine decomposition, which can be described by a typical exponential decay (eq 1).

$$N(t) = N_0 \times e^{-kt} \quad (1)$$

The photoactivation half-life $t_{1/2}$ and the time constant τ of the diazirine derivatives **3a** and **3b** were calculated from the resulting rate constant k according to eq 2 and are listed in Table 2.

$$t_{1/2} = \frac{\ln(2)}{k} = \tau \times \ln(2) \quad (2)$$

In cyclohexane and aqueous buffer, diazirine decomposition over the course of light exposure occurred immediately within a few seconds ($t_{1/2}$ 7–9 s), whereas prolonged irradiation times were required in methanol ($t_{1/2}$ 12 and 34 min for **3a** and **3b**,

Table 2. Calculated Photoactivation Half-Lives and Time Constants of the Synthesized Diazirines in Different Solvents^a

compound	methanol		cyclohexane		aqueous buffer ^b	
	$t_{1/2}$ (min)	τ (min)	$t_{1/2}$ (s)	τ (s)	$t_{1/2}$ (s)	τ (s)
3a	12	18	8	11	10	14
3b	34	49	7	9	9	12

^aDistance from UV light source ($\lambda = 365$ nm): 2 cm (see Experimental Section for details). ^b $c = 50$ μ M in 50 mM TRIS, 150 mM NaCl, 2 mM CaCl₂, 5 mM KCl, 5 mM MgCl₂, 4 mM EDTA, and 250 mM sucrose.

respectively), which is consistent with the results of the NMR experiments. Interestingly, the curves and half-lives of diazirines **3a** and **3b** in methanolic solution illustrated substantial kinetic differences indicating distinct photolytic properties between both constitution isomers, which were not observed in cyclohexane or aqueous solution. Presumably, the corresponding photochemical properties of the diazirines **3a** and **3b** can be attributed to a different stabilization of the intermediate carbenes: the empty p orbital in the case of **20b** can additionally be stabilized by the electron-donating piperidine moiety in the *para* position (Figure 7). In contrast, the electron deficiency in **20a** cannot be compensated to the same extent, resulting in higher reactivity and thus faster insertion. The carbene-stabilizing effect is probably especially enhanced by the methanolic solvent but is not as pronounced in the other solvents since the reactive intermediates are directly scavenged by solvent molecules. Similar observations have already been reported in which substituent and solvent effects on carbene reactions explained their different reactivity.^{64–67} The higher reactivity of the carbenes toward water compared to methanol can presumably be explained by the higher acidity and the extended hydrogen bonding network of water.⁶⁸

In an aqueous buffer, both modified TRPML activators cleanly underwent photolysis at 365 nm within 90 s, and product formation was completed after 360 s including a fast decay of the linear diazo compound (Figure 8).

The short irradiation times required, combined with a temporarily short-lived formation of the undesired linear diazo compound, demonstrated efficient photoactivation of (trifluoromethyl)diazirines **3a** and **3b**, respectively, highlighting their suitability for photoaffinity labeling in an aqueous environment since long irradiation periods exhibit an increased risk of unspecific labeling (pseudoaffinity labeling) or even damage of biological systems.^{31,32} These results also reveal the ability of water to quench the highly reactive carbenes immediately, which further contributes to minimizing unspecific labeling: only molecules in a close environment to the binding site of the protein will react covalently with amino acid residues, whereas free and unbound molecules are directly scavenged by the aqueous medium.³² In all photolysis experiments, no characteristic products arising from hydrogen atom abstraction (such as reduced derivatives of **3a** and **3b**) were observed, suggesting that the involvement of triplet carbene intermediates is rather unlikely. Indeed, it was previously noted that most of the products developed during photolysis of aromatic diazirines result from a singlet carbene state.^{69,70}

CONCLUSION

Two modified TRPML1 activators featuring a photoreactive (trifluoromethyl)diazirine moiety were designed and synthe-

sized. These MK6–83 analogues exhibited favorable physicochemical properties since they efficiently underwent clean photolysis to the desired insertion products, as demonstrated in detailed photoactivation studies in various solvents. Furthermore, fast diazirine decay associated with short irradiation times required in aqueous buffer additionally proves their suitability for photoaffinity labeling procedures. They were also shown to be stable during long-term storage at low temperatures in the absence of light, which highlights their value as useful and important photoreactive analogues of the TRPML1 activator MK6–83. In their crystal structures, the differences in the substitution pattern led to significant differences in the crystal packing pattern involving an unusual diazirine-CF₃ close contact. Future investigations exploiting the advantageous properties of the photoreactive analogues presented here will provide detailed insights into TRPML1 modulation by the synthetic agonist MK6–83. Biological functional analysis and photoaffinity labeling experiments in combination with a proteomics mass spectrometry approach can thus make a significant contribution to elucidating the binding site within the TRPML1 channel. This knowledge could be very important for the structure-based design of new TRPML activators and helpful to further explore the mechanism of TRPML activation by synthetic molecules.

EXPERIMENTAL SECTION

Chemistry. All solvents and reagents were obtained from commercial suppliers (Sigma-Aldrich, Acros Organics, Alfa Aesar, TCI, or Apollo Scientific) and used without any prior purification, if not stated otherwise. Anhydrous methyl *tert*-butyl ether, tetrahydrofuran, and 1,4-dioxane were freshly distilled from sodium and benzophenone. Dichloromethane was dried by distillation from calcium hydride. Reactions under anhydrous conditions were performed under an argon atmosphere using flame-dried glassware. Unless otherwise mentioned, heating was carried out with an oil bath if needed. Reactions at -78 °C were conducted in a dry ice/acetone cooling bath. Purifications by flash chromatography were performed on silica gel (0.015–0.040 mm, Machery-Nagel). Reaction progress was monitored by thin-layer chromatography (TLC) using Machery-Nagel Alugram Xtra Sil G/UV₂₅₄ silica 60 plates. Compound visualization on these plates was attained by radiation at 254 nm or by staining with Ehrlich's reagent (prepared from 4-(*N,N*-dimethylamino)benzaldehyde (1.6 g) and concentrated HCl (80 mL) in methanol (120 mL)).

¹H and ¹³C NMR spectra were recorded on a Bruker Fourier 300, a Bruker Avance-III HD (¹H NMR, 300 MHz; ¹³C{¹H} NMR, 75.5 MHz; ¹⁹F NMR, 282 MHz), or a Bruker Avance-II (¹H NMR 400 MHz; ¹³C{¹H} NMR 100.6 MHz; ¹⁹F NMR 376 MHz). Two-dimensional NMR experiments (COSY, HSQC, and HMBC) were used for assignments. All chemical shifts are referenced to the signal of the residual solvent (CDCl₃, 7.26 and 77.16 ppm; DMSO-*d*₆, 2.50 and 39.52 ppm; methanol-*d*₄, 3.31 and 49.00 ppm; cyclohexane-*d*₁₂, 1.38 and 26.43 ppm for ¹H NMR and ¹³C NMR, respectively) and reported in parts per million (ppm) relative to tetramethylsilane (TMS). For ¹⁹F NMR, chemical shifts are given in ppm relative to C(³⁵Cl)₂(³⁷Cl)F. The spectrometer was calibrated with α,α,α -trifluorotoluene in CDCl₃ (−63.9 ppm). Multiplicities of the corresponding NMR signals are given using the following abbreviations: br = broad, s = singlet, d = doublet, t = triplet, q = quartet, m = multiplet, and combinations thereof. Infrared (IR) spectra were recorded on an FT-IR spectrometer (Avatar, Thermo-Nicolet) with an ATR correction and are reported in terms of frequency of absorption $\bar{\nu}$ [cm^{−1}].

Analytical HPLC analysis was performed on an HP Agilent 1100 series HPLC system using an Agilent Poroshell 120 EC-C₁₈ (150 × 2.10 mm, 4 μ m) column at 40 °C oven temperature and a detection wavelength of 254 nm. The mobile phase consisted of mixtures of acetonitrile, Milli-Q-grade water, and 10% of a 0.1% solution of formic acid in Milli-Q-grade water and was adapted to each separation problem

(injection volume = 5–20 μL ; flow rate = 0.5–0.7 mL min^{-1}). Electrospray ionization (ESI) mass spectra were recorded on an Agilent 1100 series LC/MSD ion trap spectrometer in the positive ion mode (drying gas temperature = 350 $^{\circ}\text{C}$, nebulizer pressure = 70 psi, capillary voltage = 3500 V, drying gas (N_2) = 12 L min^{-1}). The purity of the final compounds was confirmed by HPLC analysis and was higher than 95% in all cases. Semipreparative HPLC was performed on a Varian PrepStar system using an Agilent Zorbax PrepHT XDB C_{18} (150 mm \times 21.2 mm, 5 μm) column at a detection wavelength of 254 nm. The mobile phase consisted of mixtures of acetonitrile and Milli-Q-grade water and was adapted to each separation problem (injection volume = 1–5 mL, flow rate = 10–20 mL min^{-1}). High-resolution masses (ESI-MS) were recorded using an Agilent 6545 Q-TOF-MS instrument with a suitable external calibrant. Melting points were determined in open capillaries on a Krüss-Optronic KSP 1 N apparatus (heating rate = 1 $^{\circ}\text{C/min}$).

X-ray diffraction was measured at 100 K on a Rigaku SuperNova diffractometer with a CCD Eos detector using monochromated Mo $K\alpha$ ($\lambda = 0.71073 \text{ \AA}$) radiation. Single crystals suitable for crystallography were obtained by recrystallization from a CH_2Cl_2 solution of diazirines **3a** and **3b**, respectively, with vapor diffusion of petroleum ether at room temperature.

Note that all photolabile compounds were stored in the dark under an argon atmosphere at $-21 \text{ }^{\circ}\text{C}$ to prevent decomposition.

2,2,2-Trifluoro-*N*-methoxy-*N*-methylacetamide (9). This compound was prepared according to reported procedures.^{46,47} To a mixture of *N,O*-dimethylhydroxylamine hydrochloride (7.90 g, 80.99 mmol, 1.05 equiv) and trifluoroacetic anhydride (10.9 mL, 77.14 mmol, 1.00 equiv) in CH_2Cl_2 (200 mL) was added pyridine (18.5 mL, 229.2 mmol, 2.97 equiv) dropwise at 0 $^{\circ}\text{C}$. The resulting mixture was stirred for 2 h at 0 $^{\circ}\text{C}$ and then quenched with water (50 mL). The organic layer was washed with water (1 \times 50 mL), 1 M HCl (aq) (2 \times 100 mL), and a solution of NaCl (aq) (saturated, 1 \times 100 mL) and dried over Na_2SO_4 , and the solvent was removed under reduced pressure to afford the title compound (7.74 g, 49.27 mmol, 64% yield) as a colorless oil, which was used for the next reaction without further purification. $^1\text{H NMR}$ (300 MHz, CDCl_3): δ 3.70 (s, 3H, OCH_3), 3.22 (s, 3H, NCH_3) ppm. $^{13}\text{C}\{^1\text{H}\}$ NMR (75.5 MHz, CDCl_3): δ 156.8 (q, $^2J_{\text{CF}} = 37.3 \text{ Hz}$, $\text{CF}_3\text{C}(\text{O})$), 116.2 (q, $^1J_{\text{CF}} = 286.4 \text{ Hz}$, CF_3), 62.1 (OCH_3), 32.7 (NCH_3) ppm. IR (ATR): $\bar{\nu}$ 1701, 1257, 1211, 1152, 1082, 983, 896, 745, 662 cm^{-1} .

The analytical data are consistent with those reported in the literature.⁴⁷

1-(5-Bromo-2-nitrophenyl)piperidine (11a). This compound was synthesized according to a modified procedure by Yin et al.⁴¹ To a mixture of 4-bromo-2-fluoro-1-nitrobenzene (8.00 g, 36.36 mmol, 1.00 equiv) and Cs_2CO_3 (15.04 g, 46.17 mmol, 1.27 equiv) in DMF (100 mL) was added piperidine (3.8 mL, 38.18 mmol, 1.05 equiv) at room temperature. After stirring overnight, the solvent was evaporated under reduced pressure, and the residue was dissolved in EtOAc (100 mL) and water (100 mL). The aqueous phase was extracted with EtOAc (3 \times 100 mL), and the combined organic phases were dried over Na_2SO_4 and concentrated under reduced pressure to obtain the title compound (10.29 g, 36.09 mmol, 99% yield) as an orange solid. $R_f = 0.65$ (SiO_2 , $^{\text{Hex}}/\text{EtOAc} = 10:1$). Mp: 60–61 $^{\circ}\text{C}$. $^1\text{H NMR}$, COSY (300 MHz, CDCl_3): δ 7.63 (d, $^3J = 8.7 \text{ Hz}$, 1H, $H\text{-}3^{\text{Ph}}$), 7.22 (d, $^4J = 2.0 \text{ Hz}$, 1H, $H\text{-}6^{\text{Ph}}$), 7.03 (dd, $^3J = 8.7$, $^4J = 2.0 \text{ Hz}$, 1H, $H\text{-}4^{\text{Ph}}$), 3.06–2.97 (m, 4H, 2 \times $H\text{-}2^{\text{Pip}}$ and 2 \times $H\text{-}6^{\text{Pip}}$), 1.76–1.65 (m, 4H, 2 \times $H\text{-}3^{\text{Pip}}$ and 2 \times $H\text{-}5^{\text{Pip}}$), 1.65–1.53 (m, 2H, 2 \times $H\text{-}4^{\text{Pip}}$) ppm. $^{13}\text{C}\{^1\text{H}\}$ NMR, HSQC, HMBC (75.5 MHz, CDCl_3): δ 147.8 ($\text{C}\text{-}1^{\text{Ph}}$), 140.7 ($\text{C}\text{-}2^{\text{Ph}}$), 128.1 ($\text{C}\text{-}5^{\text{Ph}}$), 127.7 ($\text{C}\text{-}3^{\text{Ph}}$), 123.9 ($\text{C}\text{-}6^{\text{Ph}}$), 123.3 ($\text{C}\text{-}4^{\text{Ph}}$), 52.8 ($\text{C}\text{-}2^{\text{Pip}}$ and $\text{C}\text{-}6^{\text{Pip}}$), 25.8 ($\text{C}\text{-}3^{\text{Pip}}$ and $\text{C}\text{-}5^{\text{Pip}}$), 23.9 ($\text{C}\text{-}4^{\text{Pip}}$) ppm. IR (ATR): $\bar{\nu}$ 2934, 2852, 1591, 1548, 1498, 1332, 1295, 1231, 1135, 1033 cm^{-1} . MS (ESI): m/z calcd for $[\text{C}_{11}\text{H}_{13}\text{BrN}_2\text{O}_2 + \text{H}]^+$ ($[\text{M} + \text{H}]^+$), 285.0/287.0; found, $m/z = 285.2$ (90%, $[\text{M} + \text{H}]^+$)/287.0 (100%, $[\text{M} + \text{H}]^+$).

The analytical data are consistent with those reported in the literature.⁷¹

4-Bromo-2-(piperidin-1-yl)aniline (12a). This compound was synthesized according to a modified procedure by Yin et al.⁴¹ To a solution of **11a** (9.24 g, 32.40 mmol, 1.00 equiv) in EtOAc (250 mL) was added $\text{SnCl}_4 \cdot 2 \text{ H}_2\text{O}$ (24.80 g, 97.20 mmol, 3.00 equiv). After

stirring overnight at room temperature, the reaction was quenched by the addition of a KF (aq) solution (1 M, 100 mL) and stirred further 30 min. The mixture was extracted with EtOAc (2 \times 250 mL). The combined organic layers were washed with a KF (aq) solution (1 M, 1 \times 100 mL) and a solution of NaCl (aq) (saturated, 2 \times 100 mL) and dried over Na_2SO_4 , and the solvent was removed under reduced pressure. The title compound was obtained as a yellow-brown solid (7.65 g, 29.98 mmol, 93% yield), which was used without any further purification. $R_f = 0.50$ (SiO_2 , $^{\text{Hex}}/\text{EtOAc} = 5:1$). Mp: 40–41 $^{\circ}\text{C}$. $^1\text{H NMR}$, COSY (300 MHz, $\text{DMSO}\text{-}d_6$): δ 6.98–6.89 (m, 2H, $H\text{-}3^{\text{Ph}}$ and $H\text{-}5^{\text{Ph}}$), 6.70–6.60 (m, 1H, $H\text{-}6^{\text{Ph}}$), 4.91 (s (br), 2H, NH_2), 2.76–2.67 (m, 4H, 2 \times $H\text{-}2^{\text{Pip}}$ and 2 \times $H\text{-}6^{\text{Pip}}$), 1.70–1.57 (m, 4H, 2 \times $H\text{-}3^{\text{Pip}}$ and 2 \times $H\text{-}5^{\text{Pip}}$), 1.56–1.44 (m, 2H, 2 \times $H\text{-}4^{\text{Pip}}$) ppm. $^{13}\text{C}\{^1\text{H}\}$ NMR, HSQC, HMBC (75.5 MHz, $\text{DMSO}\text{-}d_6$): δ 141.6 ($\text{C}\text{-}2^{\text{Ph}}$), 139.9 ($\text{C}\text{-}1^{\text{Ph}}$), 126.1 ($\text{C}\text{-}5^{\text{Ph}}$), 121.9 ($\text{C}\text{-}3^{\text{Ph}}$), 115.7 ($\text{C}\text{-}6^{\text{Ph}}$), 107.0 ($\text{C}\text{-}4^{\text{Ph}}$), 51.6 ($\text{C}\text{-}2^{\text{Pip}}$ and $\text{C}\text{-}6^{\text{Pip}}$), 26.0 ($\text{C}\text{-}3^{\text{Pip}}$ and $\text{C}\text{-}5^{\text{Pip}}$), 23.7 ($\text{C}\text{-}4^{\text{Pip}}$) ppm. IR (ATR): $\bar{\nu}$ 3423, 3330, 2936, 1601, 1487, 1438, 1272, 1226, 1029, 929, 805 cm^{-1} . HRMS (ESI-QTOF) m/z : calcd for $\text{C}_{11}\text{H}_{16}\text{BrN}_2^+$ ($[\text{M} + \text{H}]^+$), 255.0491/257.0471; found, 255.0489/257.0468.

tert-Butyl [4-bromo-2-(piperidin-1-yl)phenyl]carbamate (13a). This compound was synthesized according to a method by Bartoli et al.⁴² To a solution of 4-bromo-2-(piperidin-1-yl)aniline (**12a**, 6.79 g, 26.61 mmol, 1.00 equiv) in CH_2Cl_2 (50 mL) were added Boc_2O (8.71 g, 39.91 mmol, 1.50 equiv) and $\text{Zn}(\text{ClO}_4)_2 \cdot 6 \text{ H}_2\text{O}$ (496 mg, 1.33 mmol, 0.05 equiv). The mixture was stirred at 45 $^{\circ}\text{C}$ for 5 h in an oil bath, and then an additional portion of Boc_2O (8.71 g, 39.91 mmol, 1.50 equiv) was added and stirred for further 5 h at 45 $^{\circ}\text{C}$. After stirring overnight at room temperature, water was added (100 mL), and the aqueous phase was extracted with CH_2Cl_2 (3 \times 100 mL). The combined organic extracts were dried over Na_2SO_4 and concentrated under reduced pressure. After purification by flash chromatography on silica gel ($^{\text{Hex}}/\text{EtOAc} = 80:1$), the title compound was obtained as a light-yellow solid (7.85 g, 22.10 mmol, 83% yield). $R_f = 0.53$ (SiO_2 , $^{\text{Hex}}/\text{EtOAc} = 25:1$). Mp: 89–91 $^{\circ}\text{C}$. $^1\text{H NMR}$, COSY (300 MHz, $\text{DMSO}\text{-}d_6$): δ 7.74 (d, $^3J = 8.6 \text{ Hz}$, 1H, $H\text{-}6^{\text{Ph}}$), 7.72 (s, 1H, NH), 7.28–7.17 (m, 2H, $H\text{-}3^{\text{Ph}}$ and $H\text{-}5^{\text{Ph}}$), 2.72 (*pseudo-t*, $J \approx 5.2 \text{ Hz}$, 4H, 2 \times $H\text{-}2^{\text{Pip}}$ and 2 \times $H\text{-}6^{\text{Pip}}$), 1.74–1.58 (m, 4H, 2 \times $H\text{-}3^{\text{Pip}}$ and 2 \times $H\text{-}5^{\text{Pip}}$), 1.58–1.49 (m, 2H, 2 \times $H\text{-}4^{\text{Pip}}$), 1.46 (s, 9H, $\text{C}(\text{CH}_3)_3$) ppm. $^{13}\text{C}\{^1\text{H}\}$ NMR, HSQC, HMBC (75.5 MHz, $\text{DMSO}\text{-}d_6$): δ 152.3 ($\text{C}=\text{O}$), 144.7 ($\text{C}\text{-}2^{\text{Ph}}$), 132.4 ($\text{C}\text{-}1^{\text{Ph}}$), 126.8 ($\text{C}\text{-}5^{\text{Ph}}$), 123.5 ($\text{C}\text{-}3^{\text{Ph}}$), 120.7 ($\text{C}\text{-}6^{\text{Ph}}$), 114.7 ($\text{C}\text{-}4^{\text{Ph}}$), 79.8 ($\text{C}(\text{CH}_3)_3$), 52.6 ($\text{C}\text{-}2^{\text{Pip}}$ and $\text{C}\text{-}6^{\text{Pip}}$), 27.9 ($\text{C}(\text{CH}_3)_3$), 26.0 ($\text{C}\text{-}3^{\text{Pip}}$ and $\text{C}\text{-}5^{\text{Pip}}$), 23.4 ($\text{C}\text{-}4^{\text{Pip}}$) ppm. IR (ATR): $\bar{\nu}$ 3360, 2934, 1714, 1502, 1446, 1396, 1245, 1146, 1022, 925, 833 cm^{-1} . HRMS (ESI-QTOF) m/z : calcd for $\text{C}_{16}\text{H}_{24}\text{BrN}_2\text{O}_2^+$ ($[\text{M} + \text{H}]^+$), 355.1016/357.0995; found, 355.1010/357.0991.

tert-Butyl [2-(Piperidin-1-yl)-4-(2,2,2-trifluoroacetyl)phenyl]carbamate (14a). Under an argon atmosphere, a solution of **13a** (4.69 g, 13.20 mmol, 1.00 equiv) in anhydrous THF (25 mL) was added dropwise to a suspension of KH (30% suspension in mineral oil, 2.64 g, 19.80 mmol, 1.50 equiv) in anhydrous THF (75 mL) at 0 $^{\circ}\text{C}$. After 1 h at 0 $^{\circ}\text{C}$, the reaction mixture was cooled down to $-78 \text{ }^{\circ}\text{C}$, and a solution of $t\text{-BuLi}$ (1.6 M in pentane, 17.3 mL, 27.72 mmol, 2.10 equiv) was carefully added dropwise via cannula. After 45 min, 2,2,2-trifluoro-*N*-methoxy-*N*-methylacetamide (**9**, 4.15 g, 26.40 mmol, 2.00 equiv) was added and stirring was continued for 6 h at $-78 \text{ }^{\circ}\text{C}$. The reaction was quenched by the addition of a solution of NH_4Cl (aq) (saturated, 20 mL). Water (50 mL) and EtOAc (100 mL) were added, the phases were separated, and the aqueous layer was extracted with EtOAc (3 \times 100 mL). The combined organic phases were dried over Na_2SO_4 , and the solvent was removed under reduced pressure. After purification by flash chromatography on silica gel ($^{\text{Hex}}/\text{EtOAc} = 80:1$), the title compound was obtained as a yellow solid (3.78 g, 10.15 mmol, 77% yield). $R_f = 0.42$ (SiO_2 , $^{\text{Hex}}/\text{EtOAc} = 10:1$). Mp: 110–111 $^{\circ}\text{C}$. $^1\text{H NMR}$, COSY (300 MHz, $\text{DMSO}\text{-}d_6$): δ 8.19 (d, $^3J = 8.7 \text{ Hz}$, 1H, $H\text{-}6^{\text{Ph}}$), 8.05 (s, 1H, NH), 7.80–7.72 (m, 2H, $H\text{-}3^{\text{Ph}}$ and $H\text{-}5^{\text{Ph}}$), 2.76 (*pseudo-t*, $J \approx 5.2 \text{ Hz}$, 4H, 2 \times $H\text{-}2^{\text{Pip}}$ and 2 \times $H\text{-}6^{\text{Pip}}$), 1.82–1.64 (m, 4H, 2 \times $H\text{-}3^{\text{Pip}}$ and 2 \times $H\text{-}5^{\text{Pip}}$), 1.64–1.53 (m, 2H, 2 \times $H\text{-}4^{\text{Pip}}$), 1.50 (s, 9H, $\text{C}(\text{CH}_3)_3$) ppm. $^{13}\text{C}\{^1\text{H}\}$ NMR, HSQC, HMBC (75.5 MHz, $\text{DMSO}\text{-}d_6$): δ 177.4 (q, $^2J_{\text{CF}} = 34.0 \text{ Hz}$, $\text{CF}_3\text{C}(\text{O})$), 151.3 ($\text{C}=\text{O}$), 141.8 ($\text{C}\text{-}2^{\text{Ph}}$), 140.8 ($\text{C}\text{-}1^{\text{Ph}}$), 127.8 ($\text{C}\text{-}5^{\text{Ph}}$), 122.7 ($\text{C}\text{-}4^{\text{Ph}}$), 121.8 ($\text{C}\text{-}$

³Ph), 116.4 (q, ¹J_{CF} = 292.1 Hz, CF₃), 116.3 (C-6^{Ph}), 80.7 (C(CH₃)₃), 52.8 (C-2^{Pip} and C-6^{Pip}), 27.7 (C(CH₃)₃), 26.0 (C-3^{Pip} and C-5^{Pip}), 23.2 (C-4^{Pip}) ppm. ¹⁹F NMR (376 MHz, DMSO-*d*₆): δ -71.12 (s, CF₃) ppm. IR (ATR): $\bar{\nu}$ 2936, 2359, 1738, 1697, 1593, 1519, 1442, 1223, 1190, 1127, 1051, 908 cm⁻¹. HRMS (ESI-QTOF) *m/z*: calcd for C₁₈H₂₄F₃N₂O₃⁺ [M + H]⁺, 373.1734; found, 373.1733.

tert-Butyl (E/Z)-{2-(Piperidin-1-yl)-4-[2,2,2-trifluoro-1-(hydroxyimino)ethyl]phenyl}carbamate (15a). To a solution of **14a** (2.00 g, 5.37 mmol, 1.00 equiv) in pyridine/EtOH (37.5 mL, 2:1 v/v) was added hydroxylamine hydrochloride (448 mg, 6.44 mmol, 1.20 equiv), and the mixture was stirred for 5 h at 80 °C in an oil bath. After complete conversion of the starting material, the reaction mixture was cooled, and the solvent was removed under reduced pressure. The residue was dissolved in EtOAc (100 mL), washed with water (2 × 50 mL) and a solution of NaCl (aq) (saturated, 2 × 50 mL), and dried over Na₂SO₄, and the solvent was removed under reduced pressure. After purification by flash chromatography on silica gel (Hex/EtOAc = 8:1), the title compound was obtained as a mixture of (E/Z)-diastereomers (colorless solid, 1.84 g, 4.75 mmol, 88% yield). *R*_f = 0.33 and 0.36 (SiO₂, Hex/EtOAc = 5:1). Mp: 143–144 °C. ¹H NMR, COSY (300 MHz, DMSO-*d*₆): δ 12.90 and 12.66 (2 × s, 1H, NOH, both isomers), 7.95 and 7.93 (2 × d, *J* = 8.5 Hz, 1H, *H*-6^{Ph}, both isomers), 7.88 and 7.85 (2 × s, 1H, NH, both isomers), 7.32–7.14 (m, 2H, *H*-3^{Ph} and *H*-5^{Ph}), 2.73 (*pseudo*-q, *J* ≈ 4.9 Hz, 4H, 2 × *H*-2^{Pip} and 2 × *H*-6^{Pip}), 1.73–1.60 (m, 4H, 2 × *H*-3^{Pip} and 2 × *H*-5^{Pip}), 1.60–1.50 (m, 2H, 2 × *H*-4^{Pip}), 1.48 (s, 9H, C(CH₃)₃) ppm. ¹³C{¹H} NMR, HSQC, HMBC (75.5 MHz, DMSO-*d*₆): δ 152.2 (C=O), 144.3 (q, ²J_{CF} = 28.1 Hz, CF₃CNOH, one isomer), 144.0 (q, ²J_{CF} = 30.8 Hz, CF₃CNOH, other isomer), 142.4 and 142.2 (C-2^{Ph}, both isomers), 134.80 and 134.76 (C-1^{Ph}, both isomers), 124.9 (C-5^{Ph}, one isomer), 124.7 (C-4^{Ph}, one isomer), 124.5 (C-5^{Ph}, other isomer), 121.3 (q, ¹J_{CF} = 274.0 Hz, CF₃, one isomer), 120.9 (C-3^{Ph}, one isomer), 120.7 (C-4^{Ph}, other isomer), 120.4 (C-3^{Ph}, other isomer), 118.6 (q, ¹J_{CF} = 283.0 Hz, CF₃, other isomer), 117.9 (C-6^{Ph}), 80.04 and 80.00 (C(CH₃)₃, both isomers), 52.9 (C-2^{Pip} and C-6^{Pip}), 27.9 (C(CH₃)₃), 26.2 (C-3^{Pip} and C-5^{Pip}), 23.4 (C-4^{Pip}) ppm. ¹⁹F NMR (376 MHz, DMSO-*d*₆): δ -62.80 and -65.58 (s, CF₃, both isomers) ppm. IR (ATR): $\bar{\nu}$ 3346, 2940, 2360, 1720, 1701, 1523, 1369, 1238, 1192, 1153, 1023, 964 cm⁻¹. HRMS (ESI-QTOF) *m/z*: calcd for C₁₈H₂₅F₃N₃O₃⁺ [M + H]⁺, 388.1843; found, 388.1839.

tert-Butyl {2-(Piperidin-1-yl)-4-[3-(trifluoromethyl)diaziridin-3-yl]phenyl}carbamate (16a). Under an argon atmosphere, to a solution of the oxime **15a** (1.22 g, 3.14 mmol, 1.00 equiv) in acetone (50 mL) and triethylamine (1.3 mL, 9.42 mmol, 3.00 equiv) was added a solution of *p*-toluenesulfonyl chloride (658 mg, 3.45 mmol, 1.10 equiv) in acetone (5 mL) dropwise at 0 °C. After stirring for 3 h at 0 °C, the solvent was removed under reduced pressure (no warming!) to give the crude *O*-tosyl oxime as a yellow solid, which was immediately used for the next step without further purification. Note that the product is not stable upon warming and on silica, so it is crucial to avoid further purification and warming during evaporation to obtain higher yields.

To a cooled Schlenk flask containing liquid ammonia (approximately 50 mL) under an argon atmosphere at -78 °C was added a suspension of the crude *O*-tosyl oxime in anhydrous MTBE (25 mL) dropwise. The mixture was stirred for 5 h at -78 °C and warmed to room temperature overnight (side arm of the Schlenk flask opened to allow ammonia to evaporate slowly). The resulting suspension was diluted with MTBE (50 mL) and water (50 mL) and extracted with MTBE (3 × 50 mL). The combined organic layers were dried over Na₂SO₄ and concentrated under reduced pressure to obtain the diaziridine **16a** as a colorless solid (1.21 g, 3.13 mmol, 99% yield). *R*_f = 0.38 (SiO₂, Hex/EtOAc = 5:1). Mp: 122–123 °C. ¹H NMR, COSY (300 MHz, DMSO-*d*₆): δ 7.87 (d, 1H, *J* = 8.3 Hz, *H*-6^{Ph}), 7.81 (s, 1H, NH), 7.30–7.21 (m, 2H, *H*-3^{Ph} and *H*-5^{Ph}), 4.02 (d, *J* = 8.3 Hz, 1H, NH^{diaziridine}), 3.89 (d, *J* = 8.3 Hz, 1H, NH^{diaziridine}), 2.79–2.68 (m, 4H, 2 × *H*-2^{Pip} and 2 × *H*-6^{Pip}), 1.74–1.60 (m, 4H, 2 × *H*-3^{Pip} and 2 × *H*-5^{Pip}), 1.59–1.50 (m, 2H, 2 × *H*-4^{Pip}), 1.48 (s, 9H, C(CH₃)₃) ppm. ¹³C{¹H} NMR, HSQC, HMBC (75.5 MHz, DMSO-*d*₆): δ 152.3 (C=O), 142.4 (C-2^{Ph}), 134.1 (C-1^{Ph}), 126.4 (C-4^{Ph}), 124.6 (C-5^{Ph}), 124.2 (q, ¹J_{CF} = 278.9 Hz, CF₃), 120.5 (C-3^{Ph}), 118.2 (C-6^{Ph}), 79.9 (C(CH₃)₃), 57.1 (q, ²J_{CF} = 34.8 Hz, C_q^{diaziridine}), 52.9 (C-2^{Pip} and C-6^{Pip}), 27.9 (C(CH₃)₃), 26.2 (C-3^{Pip} and C-5^{Pip}), 23.5

(C-4^{Pip}) ppm. ¹⁹F NMR (376 MHz, DMSO-*d*₆): δ -74.98 (s, CF₃) ppm. IR (ATR): $\bar{\nu}$ 3367, 2937, 2359, 1722, 1522, 1464, 1420, 1371, 1215, 1146, 1095, 1027, 948, 831 cm⁻¹. HRMS (ESI-QTOF) *m/z*: calcd for C₁₈H₂₆F₃N₄O₂⁺ [M + H]⁺, 387.2002; found, 387.2002.

tert-Butyl {2-(Piperidin-1-yl)-4-[3-(trifluoromethyl)-3H-diaziridin-3-yl]phenyl}carbamate (17a). Note that this reaction was performed in the dark to avoid partial photolysis of the product (aluminum foil was used to cover flasks and columns). To a solution of the diaziridine **16a** (1.00 g, 2.59 mmol, 1.00 equiv) in anhydrous CH₂Cl₂ (25 mL) was added triethylamine (897 μL, 6.47 mmol, 2.50 equiv) and iodine (980 mg, 3.89 mmol, 1.50 equiv) at 0 °C. The reaction mixture was stirred 1 h at 0 °C and 1 h at room temperature. After complete conversion of the starting material, the reaction was quenched by the addition of a Na₂S₂O₃ (aq) solution (1 M, 50 mL), and the aqueous layer was extracted with CH₂Cl₂ (3 × 50 mL). The combined organic layers were dried over Na₂SO₄, and the solvent was removed under reduced pressure. After flash chromatography purification on silica gel (Hex/EtOAc = 50:1), the title compound was obtained as a colorless solid (948 mg, 2.47 mmol, 95% yield). *R*_f = 0.20 (SiO₂, Hex/EtOAc = 50:1). Mp: 46–48 °C. ¹H NMR, COSY (300 MHz, DMSO-*d*₆): δ 7.94 (d, ³*J* = 8.5 Hz, 1H, *H*-6^{Ph}), 7.85 (s, 1H, NH), 7.02 (dd, ³*J* = 8.5, ⁴*J* = 1.8 Hz, 1H, *H*-5^{Ph}), 6.92 (d, ⁴*J* = 1.8 Hz, 1H, *H*-3^{Ph}), 2.76–2.67 (m, 4H, 2 × *H*-2^{Pip} and 2 × *H*-6^{Pip}), 1.72–1.59 (m, 4H, 2 × *H*-3^{Pip} and 2 × *H*-5^{Pip}), 1.57–1.49 (m, 2H, 2 × *H*-4^{Pip}), 1.47 (s, 9H, C(CH₃)₃) ppm. ¹³C{¹H} NMR, HSQC, HMBC (75.5 MHz, DMSO-*d*₆): δ 152.2 (C=O), 143.3 (C-2^{Ph}), 135.0 (C-1^{Ph}), 122.8 (C-5^{Ph}), 122.0 (q, ¹J_{CF} = 274.8 Hz, CF₃), 121.6 (C-4^{Ph}), 119.1 (C-6^{Ph}), 118.4 (C-3^{Ph}), 80.2 (C(CH₃)₃), 52.6 (C-2^{Pip} and C-6^{Pip}), 28.0 (q, ²J_{CF} = 39.8 Hz, C_q^{diaziridine}), 27.9 (C(CH₃)₃), 26.1 (C-3^{Pip} and C-5^{Pip}), 23.4 (C-4^{Pip}) ppm. ¹⁹F NMR (282 MHz, DMSO-*d*₆): δ -65.88 (CF₃) ppm. IR (ATR): $\bar{\nu}$ 3357, 2932, 1723, 1584, 1523, 1421, 1364, 1245, 1143, 1046, 979, 830 cm⁻¹. HRMS (ESI-QTOF) *m/z*: calcd for C₁₈H₂₄F₃N₄O₂⁺ [M + H]⁺, 385.1846; found, 385.1848.

2-(Piperidin-1-yl)-4-[3-(trifluoromethyl)-3H-diaziridin-3-yl]aniline hydrochloride (18a). Note that this reaction was performed in the dark to avoid partial photolysis of the product (aluminum foil was used to cover flasks and columns). Under an argon atmosphere, diaziridine **17a** (1.20 g, 3.12 mmol, 1.00 equiv) was submitted in a round-bottom flask and a hydrogen chloride solution (4.0 M in 1,4-dioxane, 15 mL) was added at room temperature. After stirring for 2 h, the solvent was removed under reduced pressure and the residue dried in a fine vacuum to obtain the title compound (998 mg, 3.11 mmol, quant) as a colorless solid, which was used without further purification in the next step. *R*_f = 0.41 (SiO₂, Hex/EtOAc = 10:1). Mp: decomposition ≥ 200 °C. ¹H NMR, COSY (300 MHz, methanol-*d*₄): δ 7.34–7.26 (m, 2H, *H*-3^{Ph} and *H*-5^{Ph}), 7.14 (d, ³*J* = 8.3 Hz, 1H, *H*-6^{Ph}), 3.54 (*pseudo*-t, *J* ≈ 5.6 Hz, 4H, 2 × *H*-2^{Pip} and 2 × *H*-6^{Pip}), 2.20–2.05 (m, 4H, 2 × *H*-3^{Pip} and 2 × *H*-5^{Pip}), 1.86–1.70 (m, 2H, 2 × *H*-4^{Pip}) ppm. ¹³C{¹H} NMR, HSQC, HMBC (75.5 MHz, methanol-*d*₄): δ 141.5 (C-1^{Ph}), 132.0 (C-2^{Ph}), 129.8 (C-5^{Ph}), 123.5 (q, ¹J_{CF} = 273.7 Hz, CF₃), 121.8 (C-3^{Ph}), 121.3 (C-6^{Ph}), 121.2 (C-4^{Ph}), 56.3 (C-2^{Pip} and C-6^{Pip}), 29.2 (q, ²J_{CF} = 40.6 Hz, C_q^{diaziridine}), 24.8 (C-3^{Pip} and C-5^{Pip}), 22.6 (C-4^{Pip}) ppm. ¹⁹F NMR (376 MHz, methanol-*d*₄): δ -68.72 (s, CF₃) ppm. IR (ATR): $\bar{\nu}$ 3418, 3154, 2400, 1655, 1524, 1317, 1244, 1148, 1137, 997, 820 cm⁻¹. HRMS (ESI-QTOF) *m/z*: calcd for C₁₈H₂₄F₃N₄O₂⁺ [M + H]⁺, 285.1322; found, 285.1315.

5-Methyl-N-[2'-(piperidin-1-yl)-4'-[3-(trifluoromethyl)-3H-diaziridin-3-yl]phenyl]thiophene-2-sulfonamide (MK6-83^{PRG1}, 3a). Note that this reaction was performed in the dark to avoid partial photolysis of the product (aluminum foil was used to cover flasks and columns). Under an argon atmosphere, 5-methylthiophene-2-sulfonyl chloride (574 mg, 2.92 mmol, 1.00 equiv) was added dropwise to a solution of **18a** (935 mg, 2.92 mmol, 1.00 equiv) in anhydrous pyridine (10 mL) at 0 °C. The mixture was stirred 1 h at 0 °C and at room temperature overnight. The solvent was removed under reduced pressure and the residue dissolved in EtOAc (100 mL). The organic layer was washed with a NH₄Cl (aq) solution (saturated, 1 × 50 mL) and a solution of NaCl (aq) (saturated, 2 × 50 mL), dried over Na₂SO₄, and concentrated under reduced pressure. After purification by column chromatography on silica gel (Hex/EtOAc = 30:1), the title compound

was isolated as a light-yellow solid (824 mg, 1.85 mmol, 63% yield). In general, no further purification was required in this step. However, if necessary, preparative HPLC purification (C_{18} , eluent A = Milli-Q-grade water, eluent B = acetonitrile, isocratic (20:80) over 90 min with a flow rate of 12.5 mL min^{-1} and detection at 254 nm) can be performed. $R_f = 0.15$ (SiO_2 , Hex/EtOAc = 20:1). Mp: 92–94 °C. $^1\text{H NMR}$, COSY (400 MHz, $\text{DMSO}-d_6$): δ 9.07 (s, 1H, NH), 7.47 (d, $^3J = 8.6$ Hz, 1H, $H-6^{\text{Ph}}$), 7.27 (d, $^3J = 3.7$ Hz, 1H, $H-3^{\text{Thio}}$), 7.03 (ddd, $^3J = 8.6$ Hz, $^4J = 2.2$ Hz, $J = 1.0$ Hz, 1H, $H-5^{\text{Ph}}$), 6.89 (d, $^4J = 2.2$ Hz, 1H, $H-3^{\text{Ph}}$), 6.86 (dd, $^3J = 3.7$ Hz, $^4J = 1.1$ Hz, 1H, $H-4^{\text{Thio}}$), 2.59–2.52 (m, 4H, $2 \times H-2^{\text{Pip}}$ and $2 \times H-6^{\text{Pip}}$), 2.45 (d, $^4J = 1.1$ Hz, 3H, CH_3), 1.67–1.57 (m, 4H, $2 \times H-3^{\text{Pip}}$ and $2 \times H-5^{\text{Pip}}$), 1.52–1.42 (m, 2H, $2 \times H-4^{\text{Pip}}$) ppm. $^{13}\text{C}\{^1\text{H}\}$ NMR, HSQC, HMBC (100.6 MHz, $\text{DMSO}-d_6$): δ 148.1 ($C-2^{\text{Thio}}$), 145.6 ($C-2^{\text{Ph}}$), 136.9 ($C-5^{\text{Thio}}$), 133.8 ($C-1^{\text{Ph}}$), 133.1 ($C-3^{\text{Thio}}$), 126.4 ($C-4^{\text{Thio}}$), 123.8 ($C-4^{\text{Ph}}$), 122.8 ($C-5^{\text{Ph}}$), 121.9 (q, $^1J_{\text{CF}} = 274.8$ Hz, CF_3), 120.7 ($C-6^{\text{Ph}}$), 119.2 ($C-3^{\text{Ph}}$), 52.8 ($C-2^{\text{Pip}}$ and $C-6^{\text{Pip}}$), 27.9 (q, $^2J_{\text{CF}} = 39.9$ Hz, $\text{C}_q^{\text{diazirine}}$), 25.6 ($C-3^{\text{Pip}}$ and $C-5^{\text{Pip}}$), 23.4 ($C-4^{\text{Pip}}$), 15.1 (CH_3) ppm. $^{19}\text{F NMR}$ (376 MHz, $\text{DMSO}-d_6$): δ -65.79 (CF_3) ppm. IR (ATR): $\bar{\nu}$ 2938, 2855, 1505, 1440, 1342, 1245, 1153, 1123, 1022, 905, 823 cm^{-1} . HRMS (ESI-QTOF) m/z : calcd for $\text{C}_{18}\text{H}_{20}\text{F}_3\text{N}_4\text{O}_2\text{S}_2^+ [\text{M} + \text{H}]^+$, 445.0974; found, 445.0972. HPLC analysis: retention time = 2.51 min; peak area = 99.80%; eluent A = Milli-Q-grade water; eluent B = CH_3CN ; eluent C = 0.1% solution of formic acid in Milli-Q-grade water; isocratic (10:80:10) over 8 min with a flow rate of 0.7 mL min^{-1} and detection at 254 nm; injection volume = 5 μL ; column temperature = 40 °C.

1-(4-Bromo-2-nitrophenyl)piperidine (11b). This compound was synthesized according to a modified procedure by Yin et al.⁴¹ To a mixture of 4-bromo-1-fluoro-2-nitrobenzene (20.00 g, 90.91 mmol, 1.00 equiv) and Cs_2CO_3 (44.43 g, 136.37 mmol, 1.50 equiv) in DMF (200 mL) was added piperidine (9.4 mL, 95.45 mmol, 1.05 equiv) at room temperature. After stirring for 1 h, the solvent was evaporated under reduced pressure, and the residue was dissolved in EtOAc (200 mL) and a NaCl (aq) solution (saturated, 200 mL). The aqueous phase was extracted with EtOAc (3×200 mL), and the combined organic layers were washed with a solution of NaCl (aq) (saturated, 1×200 mL), dried over Na_2SO_4 , and concentrated under reduced pressure to obtain the title compound (25.80 g, 90.87 mmol, 99% yield) as a bright red oil, which crystallizes upon freezing to give red crystals. $R_f = 0.49$ (SiO_2 , Hex/EtOAc = 20:1). Mp: 51–52 °C. $^1\text{H NMR}$, COSY (300 MHz, $\text{DMSO}-d_6$): δ 7.98 (d, $^4J = 2.5$ Hz, 1H, $H-3^{\text{Ph}}$), 7.69 (dd, $^3J = 8.9$ Hz, $^4J = 2.5$ Hz, 1H, $H-5^{\text{Ph}}$), 7.23 (d, $^3J = 8.9$ Hz, 1H, $H-6^{\text{Ph}}$), 3.01–2.89 (m, 4H, $2 \times H-2^{\text{Pip}}$ and $2 \times H-6^{\text{Pip}}$), 1.65–1.45 (m, 6H, $2 \times H-3^{\text{Pip}}$, $2 \times H-5^{\text{Pip}}$ and $2 \times H-4^{\text{Pip}}$) ppm. $^{13}\text{C}\{^1\text{H}\}$ NMR, HSQC, HMBC (75.5 MHz, $\text{DMSO}-d_6$): δ 145.2 ($C-1^{\text{Ph}}$), 142.5 ($C-2^{\text{Ph}}$), 136.1 ($C-5^{\text{Ph}}$), 127.6 ($C-3^{\text{Ph}}$), 123.3 ($C-6^{\text{Ph}}$), 111.4 ($C-4^{\text{Ph}}$), 52.1 ($C-2^{\text{Pip}}$ and $C-6^{\text{Pip}}$), 25.4 ($C-3^{\text{Pip}}$ and $C-5^{\text{Pip}}$), 23.3 ($C-4^{\text{Pip}}$) ppm. IR (ATR): $\bar{\nu}$ 2933, 2814, 1598, 1506, 1448, 1324, 1281, 1224, 1127, 1022, 828 cm^{-1} . MS (ESI): m/z calcd for $[\text{C}_{11}\text{H}_{13}\text{BrN}_2\text{O}_2 + \text{H}]^+ [\text{M} + \text{H}]^+$, 285.0/287.0; found, $m/z = 285.1$ (87%, $[\text{M} + \text{H}]^+$)/287.0 (100%, $[\text{M} + \text{H}]^+$).

The analytical data are consistent with those reported to the literature.⁷³

5-Bromo-2-(piperidin-1-yl)aniline (12b). This compound was synthesized according to a modified procedure by Yin et al.⁴¹ To a solution of **11b** (10.00 g, 35.21 mmol, 1.00 equiv) in EtOAc (250 mL) was added $\text{SnCl}_4 \cdot 2\text{H}_2\text{O}$ (27.00 g, 105.63 mmol, 3.00 equiv) at room temperature. After stirring for 1 h, the reaction was quenched by the addition of a KF (aq) solution (2 M, 200 mL) and stirred further 30 min. The phases were separated, and the aqueous layer was extracted with EtOAc (3×100 mL). The combined organic extracts were washed with a KF (aq) solution (1 M, 1×100 mL) and a solution of NaCl (aq) (saturated, 2×100 mL), dried over Na_2SO_4 , and concentrated under reduced pressure. The title compound was obtained as a yellow solid (8.64 g, 33.86 mmol, 96% yield), which was used without any further purification. $R_f = 0.43$ (SiO_2 , Hex/EtOAc = 20:1). Mp: 71–73 °C. $^1\text{H NMR}$, COSY (300 MHz, $\text{DMSO}-d_6$): δ 6.82 (d, $^4J = 2.3$ Hz, 1H, $H-6^{\text{Ph}}$), 6.76 (d, $^3J = 8.3$ Hz, 1H, $H-3^{\text{Ph}}$), 6.63 (dd, $^3J = 8.3$, $^4J = 2.4$ Hz, 1H, $H-4^{\text{Ph}}$), 4.96 (s (br), 2H, NH_2), 2.69 (*pseudo-t*, $J \approx 5.1$ Hz, 4H, $2 \times H-2^{\text{Pip}}$ and $2 \times H-6^{\text{Pip}}$), 1.63 (*pseudo-p*, $J \approx 5.5$ Hz, 4H, $2 \times H-3^{\text{Pip}}$ and $2 \times H-5^{\text{Pip}}$), 1.55–1.43 (m, 2H, $2 \times H-4^{\text{Pip}}$). $^{13}\text{C}\{^1\text{H}\}$ NMR, HSQC,

HMBC (75.5 MHz, $\text{DMSO}-d_6$): δ 144.3 ($C-1^{\text{Ph}}$), 138.6 ($C-2^{\text{Ph}}$), 121.0 ($C-3^{\text{Ph}}$), 118.5 ($C-4^{\text{Ph}}$), 116.0 (2C , $C-5^{\text{Ph}}$ and $C-6^{\text{Ph}}$), 51.7 ($C-2^{\text{Pip}}$ and $C-6^{\text{Pip}}$), 26.1 ($C-3^{\text{Pip}}$ and $C-5^{\text{Pip}}$), 23.9 ($C-4^{\text{Pip}}$) ppm. IR (ATR): $\bar{\nu}$ 3443, 3343, 2932, 2794, 1593, 1495, 1379, 1229, 1200, 843, 795 cm^{-1} . HRMS (ESI-QTOF) m/z : calcd for $\text{C}_{11}\text{H}_{16}\text{BrN}_2^+ [\text{M} + \text{H}]^+$, 255.0491/257.0471; found, 255.0493/257.0473.

tert-Butyl [5-Bromo-2-(piperidin-1-yl)phenyl]carbamate (13b). This compound was synthesized according to a method by Kelly et al.⁴³ Under an argon atmosphere, a solution of NaHMDS (1.9 M in THF, 25.0 mL, 47.02 mmol, 2.00 equiv) was added dropwise to a solution of the aniline **12b** (6.00 g, 23.51 mmol, 1.00 equiv) in anhydrous THF (25 mL) at room temperature. After stirring for 15 min, a solution of Boc_2O (5.13 g, 23.51 mmol, 1.00 equiv) in anhydrous THF (5 mL) was added, and the reaction mixture was stirred overnight. NH_4Cl (aq) (saturated, 20 mL) was added to quench the reaction, the solvent was removed under reduced pressure, and the aqueous layer was extracted with EtOAc (3×100 mL). The combined organic layers were dried over Na_2SO_4 , concentrated under reduced pressure, and purified by flash chromatography on silica gel (Hex/EtOAc = 80:1) to obtain the title compound as a red oil, which crystallizes upon freezing (5.04 g, 14.19 mmol, 60% yield). $R_f = 0.53$ (SiO_2 , Hex/EtOAc = 20:1). Mp: 83–85 °C. $^1\text{H NMR}$, COSY (300 MHz, $\text{DMSO}-d_6$): δ 8.03 (d, $^4J = 2.3$ Hz, 1H, $H-6^{\text{Ph}}$), 7.80 (s, 1H, NH), 7.16 (dd, $^3J = 8.5$, $^4J = 2.3$ Hz, 1H, $H-4^{\text{Ph}}$), 7.10 (d, $^3J = 8.5$ Hz, 1H, $H-3^{\text{Ph}}$), 2.69 (*pseudo-t*, $J \approx 5.2$ Hz, 4H, $2 \times H-2^{\text{Pip}}$ and $2 \times H-6^{\text{Pip}}$), 1.71–1.58 (m, 4H, $2 \times H-3^{\text{Pip}}$ and $2 \times H-5^{\text{Pip}}$), 1.58–1.48 (m, 2H, $2 \times H-4^{\text{Pip}}$), 1.47 (s, 9H, $\text{C}(\text{CH}_3)_3$) ppm. $^{13}\text{C}\{^1\text{H}\}$ NMR, HSQC, HMBC (75.5 MHz, $\text{DMSO}-d_6$): δ 152.2 ($\text{C}=\text{O}$), 141.8 ($C-2^{\text{Ph}}$), 134.6 ($C-1^{\text{Ph}}$), 125.3 ($C-4^{\text{Ph}}$), 122.7 ($C-3^{\text{Ph}}$), 120.6 ($C-6^{\text{Ph}}$), 116.5 ($C-5^{\text{Ph}}$), 80.2 ($\text{C}(\text{CH}_3)_3$), 52.8 ($C-2^{\text{Pip}}$ and $C-6^{\text{Pip}}$), 27.9 ($\text{C}(\text{CH}_3)_3$), 26.1 ($C-3^{\text{Pip}}$ and $C-5^{\text{Pip}}$), 23.4 ($C-4^{\text{Pip}}$) ppm. IR (ATR): $\bar{\nu}$ 3443, 3343, 2932, 2814, 2358, 1718, 1593, 1495, 1437, 1228, 1026, 843, 796 cm^{-1} . HRMS (ESI-QTOF) m/z : calcd for $\text{C}_{16}\text{H}_{24}\text{BrN}_2\text{O}_2^+ [\text{M} + \text{H}]^+$, 355.1016/357.0995; found, 355.1016/357.0997.

tert-Butyl [2-(Piperidin-1-yl)-5-(2,2,2-trifluoroacetyl)phenyl]carbamate (14b). Under an argon atmosphere, a solution of **13b** (4.74 g, 13.34 mmol, 1.00 equiv) in anhydrous THF (25 mL) was added dropwise to a suspension of KH (30% suspension in mineral oil, 2.68 g, 20.01 mmol, 1.50 equiv) in anhydrous THF (100 mL) at 0 °C. After 1 h at 0 °C, the reaction mixture was cooled down to -78 °C and a solution of $^t\text{BuLi}$ (1.9 M in pentane, 14.7 mL, 28.01 mmol, 2.10 equiv) was carefully added dropwise via cannula. After 60 min, 2,2,2-trifluoro-*N*-methoxy-*N*-methylacetamide (**9**, 4.19 g, 26.68 mmol, 2.00 equiv) was added and stirring was continued for 6 h at -78 °C. The reaction was quenched by the addition of a solution of NH_4Cl (aq) (saturated, 25 mL). Water (50 mL) and EtOAc (100 mL) were added, the phases were separated, and the aqueous layer was extracted with EtOAc (3×100 mL). The combined organic phases were dried over Na_2SO_4 , and the solvent was removed under reduced pressure. After purification by flash chromatography on silica gel (Hex/EtOAc = 30:1), the title compound was obtained as a light-yellow solid (3.26 g, 8.76 mmol, 66% yield). Note that the product may be in equilibrium with its hydrate form ($\approx 3.0\text{--}1.5\text{:}1$, determined by $^1\text{H NMR}$ spectroscopy). $R_f = 0.18$ (SiO_2 , Hex/EtOAc = 20:1). Mp: 106–107 °C. $^1\text{H NMR}$, COSY (300 MHz, $\text{DMSO}-d_6$): δ 8.21 (d, $^4J = 2.3$ Hz, 1H, $H-6^{\text{Ph}}$), 8.04 (s, 1H, NH), 7.73 (ddq, $^3J = 8.6$ Hz, $^4J = 2.3$ Hz, $J = 1.4$ Hz, 1H, $H-4^{\text{Ph}}$), 7.22 (d, $^3J = 8.6$ Hz, 1H, $H-3^{\text{Ph}}$), 3.03–2.93 (m, 4H, $2 \times H-2^{\text{Pip}}$ and $2 \times H-6^{\text{Pip}}$), 1.80–1.62 (m, 4H, $2 \times H-3^{\text{Pip}}$ and $2 \times H-5^{\text{Pip}}$), 1.62–1.52 (m, 2H, $2 \times H-4^{\text{Pip}}$), 1.47 (s, 9H, $\text{C}(\text{CH}_3)_3$) ppm. $^{13}\text{C}\{^1\text{H}\}$ NMR, HSQC, HMBC (75.5 MHz, $\text{DMSO}-d_6$): δ 178.0 (q, $^2J_{\text{CF}} = 33.5$ Hz, $\text{CF}_3\text{C}(\text{O})$), 152.8 ($\text{C}=\text{O}$), 152.0 ($C-2^{\text{Ph}}$), 131.4 ($C-1^{\text{Ph}}$), 127.0 ($C-4^{\text{Ph}}$), 123.9 ($C-6^{\text{Ph}}$), 122.4 ($C-5^{\text{Ph}}$), 119.8 ($C-3^{\text{Ph}}$), 116.7 (q, $^1J_{\text{CF}} = 292.0$ Hz, CF_3), 79.8 ($\text{C}(\text{CH}_3)_3$), 51.3 ($C-2^{\text{Pip}}$ and $C-6^{\text{Pip}}$), 28.0 ($\text{C}(\text{CH}_3)_3$), 25.5 ($C-3^{\text{Pip}}$ and $C-5^{\text{Pip}}$), 23.6 ($C-4^{\text{Pip}}$) ppm. $^{19}\text{F NMR}$ (282 MHz, $\text{DMSO}-d_6$): δ -71.13 (CF_3) ppm. IR (ATR): $\bar{\nu}$ 2945, 1731, 1699, 1599, 1527, 1442, 1239, 1138, 1127, 1103, 917, 767, 734, 657 cm^{-1} . HRMS (ESI-QTOF) m/z : calcd for $\text{C}_{18}\text{H}_{24}\text{F}_3\text{N}_2\text{O}_3^+ [\text{M} + \text{H}]^+$, 373.1734; found, 373.1732.

tert-Butyl (E/Z)-{2-(Piperidin-1-yl)-5-[2,2,2-trifluoro-1-(hydroxyimino)ethyl]phenyl}carbamate (15b). To a solution of **14b** (3.06 g, 8.22 mmol, 1.00 equiv) in pyridine/EtOH (60 mL, 2:1 v/v) was added hydroxylamine hydrochloride (685 mg, 9.86 mmol, 1.20

equiv), and the mixture was stirred for 4 h at 80 °C in an oil bath. After complete conversion of the starting material, the reaction mixture was cooled, and the solvent removed under reduced pressure. The residue was dissolved in EtOAc (100 mL), washed with a solution of NH₄Cl (aq) (saturated, 1 × 50 mL), water (1 × 50 mL), and a solution of NaCl (aq) (saturated, 1 × 50 mL), and dried over Na₂SO₄, and the solvent was removed under reduced pressure. The title compound was obtained as a mixture of (*E/Z*)-diastereomers (colorless solid, 3.07 g, 7.92 mmol, 96% yield). *R*_f = 0.32 (SiO₂, ⁴Hex/EtOAc = 5:1). Mp: 69–72 °C. ¹H NMR, COSY (300 MHz, DMSO-*d*₆): δ 12.95 and 12.67 (2 × s, 1H, NOH, both isomers), 7.98 and 7.95 (2 × d, ⁴*J* = 2.0 Hz, 1H, *H*-6^{Ph}, both isomers), 7.77 and 7.75 (2 × s, 1H, NH, both isomers), 7.21 and 7.18 (2 × d, ³*J* = 8.2 Hz, 1H, *H*-3^{Ph}, both isomers), 7.15–7.08 (m, 1H, *H*-4^{Ph}), 2.76 (*pseudo-q*, *J* ≈ 4.8 Hz, 4H, 2 × *H*-2^{Pip} and 2 × *H*-6^{Pip}), 1.73–1.59 (m, 4H, 2 × *H*-3^{Pip} and 2 × *H*-5^{Pip}), 1.59–1.48 (m, 2H, 2 × *H*-4^{Pip}), 1.46 (2 × s, 9H, C(CH₃)₃, both isomers) ppm. ¹³C{¹H} NMR, HSQC, HMBC (75.5 MHz, DMSO-*d*₆): δ 152.4 (C=O), 144.49 and 144.36 (C-2^{Ph}, both isomers), 144.41 (q, ²*J*_{CF} = 28.1 Hz, CF₃CNOH, one isomer) and 144.40 (q, ²*J*_{CF} = 31.0 Hz, CF₃CNOH, other isomer), 132.8 and 132.7 (C-1^{Ph}, both isomers), 126.0 (C-5^{Ph}, one isomer), 123.5 and 122.9 (C-4^{Ph}, both isomers), 122.0 (C-5^{Ph}, other isomer), 121.2 (q, ¹*J*_{CF} = 274.2 Hz, CF₃, one isomer), 120.34 and 120.31 (C-3^{Ph}, both isomers), 119.2 and 118.58 (C-6^{Ph}, both isomers), 118.56 (q, ¹*J*_{CF} = 283.0 Hz, CF₃, both isomers), 79.9 and 79.8 (C(CH₃)₃, both isomers), 52.6 and 52.5 (C-2^{Pip} and C-6^{Pip}, both isomers), 27.9 (C(CH₃)₃), 26.0 (C-3^{Pip} and C-5^{Pip}), 23.5 (C-4^{Pip}) ppm. ¹⁹F NMR (376 MHz, DMSO-*d*₆): δ –62.78 and –65.86 (s, CF₃, both isomers) ppm. IR (ATR): $\bar{\nu}$ 3331, 2938, 1681, 1522, 1444, 1369, 1235, 1150, 1128, 1105, 1023, 978, 821, 719 cm⁻¹. HRMS (ESI-QTOF) *m/z*: calcd for C₁₈H₂₅F₃N₃O₃⁺ [M + H]⁺, 388.1843; found, 388.1844.

tert-Butyl (2-(Piperidin-1-yl)-5-[3-(trifluoromethyl)diaziridin-3-yl]phenyl)carbamate (16b). Under an argon atmosphere, to a solution of the oxime **15b** (3.05 g, 7.87 mmol, 1.00 equiv) in acetone (80 mL) and triethylamine (3.3 mL, 23.61 mmol, 3.00 equiv) was added a solution of *p*-toluenesulfonyl chloride (1.65 g, 8.66 mmol, 1.10 equiv) in acetone (10 mL) dropwise at 0 °C. After stirring for 3 h at 0 °C, the solvent was removed under reduced pressure (no warming!) to give the crude *O*-tosyl oxime as a yellow solid, which was immediately used for the next step without further purification. Note that the product is not stable upon warming and on silica, so it is crucial to avoid further purification and warming during evaporation to obtain higher yields.

To a cooled Schlenk flask containing liquid ammonia (approximately 100 mL) under an argon atmosphere at –78 °C was added a suspension of the crude *O*-tosyl oxime in anhydrous MTBE (75 mL) dropwise. The mixture was stirred for 6 h at –78 °C and warmed to room temperature overnight (side arm of the Schlenk flask opened to allow ammonia to evaporate slowly). The resulting suspension was diluted with MTBE (100 mL) and water (100 mL) and extracted with MTBE (3 × 100 mL). The combined organic layers were dried over Na₂SO₄ and concentrated under reduced pressure to obtain the diaziridine **16b** as a colorless amorphous solid (2.61 g, 6.75 mmol, 86% yield). *R*_f = 0.33 (SiO₂, ⁴Hex/EtOAc = 5:1). ¹H NMR, COSY (300 MHz, DMSO-*d*₆): δ 8.10 (d, ⁴*J* = 1.8 Hz, 1H, *H*-6^{Ph}), 7.77 (s, 1H, NH), 7.25–7.12 (m, 2H, *H*-3^{Ph} and *H*-4^{Ph}), 4.02 (d, ³*J* = 8.2 Hz, 1H, NH^{diaziridine}), 3.88 (d, ³*J* = 8.2 Hz, 1H, NH^{diaziridine}), 2.73 (*pseudo-t*, *J* ≈ 5.2 Hz, 4H, 2 × *H*-2^{Pip} and 2 × *H*-6^{Pip}), 1.73–1.60 (m, 4H, 2 × *H*-3^{Pip} and 2 × *H*-5^{Pip}), 1.60–1.49 (m, 2H, 2 × *H*-4^{Pip}), 1.48 (s, 9H, C(CH₃)₃) ppm. ¹³C{¹H} NMR, HSQC, HMBC (75.5 MHz, DMSO-*d*₆): δ 152.3 (C=O), 143.7 (C-2^{Ph}), 132.8 (C-1^{Ph}), 127.9 (C-5^{Ph}), 124.2 (q, ¹*J*_{CF} = 278.6 Hz, CF₃), 123.1 (C-4^{Ph}), 120.3 (C-3^{Ph}), 118.6 (C-6^{Ph}), 79.8 (C(CH₃)₃), 57.3 (q, ²*J*_{CF} = 34.8 Hz, C^{diaziridine}), 52.7 (C-2^{Pip} and C-6^{Pip}), 27.9 (C(CH₃)₃), 26.1 (C-3^{Pip} and C-5^{Pip}), 23.5 (C-4^{Pip}) ppm. ¹⁹F NMR (282 MHz, DMSO-*d*₆): δ –74.98 ppm. IR (ATR): $\bar{\nu}$ 3258, 2936, 1725, 1581, 1524, 1443, 1368, 1231, 1211, 1140, 1104, 1049, 1024, 819, 709 cm⁻¹. HRMS (ESI-QTOF) *m/z*: calcd for C₁₈H₂₆F₃N₄O₂⁺ [M + H]⁺, 387.2002; found, 387.2005.

tert-Butyl (2-(Piperidin-1-yl)-5-[3-(trifluoromethyl)-3H-diaziridin-3-yl]phenyl)carbamate (17b). Note that this reaction was performed in the dark to avoid partial photolysis of the product (aluminum foil was used to cover flasks and columns). To a solution of the diaziridine **16b** (2.44 g, 6.31 mmol, 1.00 equiv) in anhydrous CH₂Cl₂ (70 mL) was

added triethylamine (2.2 mL, 15.79 mmol, 2.50 equiv) and iodine (2.39 g, 9.47 mmol, 1.50 equiv) at 0 °C. The reaction mixture was stirred 1 h at 0 °C and 1 h at room temperature. After complete conversion of the starting material, the reaction was quenched by the addition of a Na₂S₂O₃ (aq) solution (1 M, 50 mL) and the aqueous layer was extracted with CH₂Cl₂ (3 × 100 mL). The combined organic layers were dried over Na₂SO₄ and the solvent was removed under reduced pressure. After flash chromatography purification on silica gel (⁴Hex/EtOAc = 100:1), the title compound was obtained as a bright yellow solid (2.00 g, 5.20 mmol, 82% yield). *R*_f = 0.33 (SiO₂, ⁴Hex/EtOAc = 50:1). Mp: 56–58 °C. ¹H NMR, COSY (300 MHz, DMSO-*d*₆): δ 7.82–7.74 (m, 2H, *H*-6^{Ph} and NH), 7.22 (d, ³*J* = 8.4 Hz, 1H, *H*-3^{Ph}), 6.86 (dd, ³*J* = 8.3, ⁴*J* = 2.4 Hz, 1H, *H*-4^{Ph}), 2.72 (*pseudo-t*, *J* ≈ 5.2 Hz, 4H, 2 × *H*-2^{Pip} and 2 × *H*-6^{Pip}), 1.71–1.58 (m, 4H, 2 × *H*-3^{Pip} and 2 × *H*-5^{Pip}), 1.58–1.49 (m, 2H, 2 × *H*-4^{Pip}), 1.47 (s, 9H, C(CH₃)₃) ppm. ¹³C{¹H} NMR, HSQC, HMBC (75.5 MHz, DMSO-*d*₆): δ 152.3 (C=O), 144.5 (C-2^{Ph}), 133.6 (C-1^{Ph}), 122.6 (C-5^{Ph}), 122.0 (q, ¹*J*_{CF} = 274.8 Hz, CF₃), 121.3 (C-3^{Ph}), 121.1 (C-4^{Ph}), 116.2 (C-6^{Ph}), 80.2 (C(CH₃)₃), 52.5 (C-2^{Pip} and C-6^{Pip}), 28.1 (q, ²*J*_{CF} = 39.9 Hz, C^{diaziridine}), 27.9 (C(CH₃)₃), 26.0 (C-3^{Pip} and C-5^{Pip}), 23.5 (C-4^{Pip}) ppm. ¹⁹F NMR (282 MHz, DMSO-*d*₆): δ –65.85 (CF₃) ppm. IR (ATR): $\bar{\nu}$ 3356, 2940, 1729, 1525, 1440, 1366, 1252, 1148, 1106, 1049, 989, 894, 806 cm⁻¹. HRMS (ESI-QTOF) *m/z*: calcd for C₁₈H₂₄F₃N₄O₂⁺ [M + H]⁺, 385.1846; found, 385.1847.

2-(Piperidin-1-yl)-5-[3-(trifluoromethyl)-3H-diaziridin-3-yl]aniline hydrochloride (18b). Note that this reaction was performed in the dark to avoid partial photolysis of the product (aluminum foil was used to cover flasks and columns). Under an argon atmosphere, the diazirine **17b** (1.20 g, 3.12 mmol, 1.00 equiv) was submitted in a round-bottom flask and a hydrogen chloride solution (4.0 M in 1,4-dioxane, 15 mL) was added at room temperature. After stirring for 1 h, the solvent was removed under reduced pressure and the residue dried in a fine vacuum to obtain the title compound (1.00 g, 3.12 mmol, quant) as a yellow oil, which was used without further purification in the next step. *R*_f = 0.59 (SiO₂, ⁴Hex/EtOAc = 10:1). ¹H NMR, COSY (300 MHz, methanol-*d*₄): δ 7.58 (d, ³*J* = 8.7 Hz, 1H, *H*-3^{Ph}), 6.94 (d, ⁴*J* = 2.2 Hz, 1H, *H*-6^{Ph}), 6.80 (dd, ³*J* = 8.7 Hz, ⁴*J* = 2.2 Hz, 1H, *H*-4^{Ph}), 3.52–3.43 (m, 4H, 2 × *H*-2^{Pip} and 2 × *H*-6^{Pip}), 2.15–2.01 (m, 4H, 2 × *H*-3^{Pip} and 2 × *H*-5^{Pip}), 1.83–1.69 (m, 2H, 2 × *H*-4^{Pip}) ppm. ¹³C{¹H} NMR, HSQC, HMBC (75.5 MHz, methanol-*d*₄): δ 139.9 (C-1^{Ph}), 134.6 (C-2^{Ph}), 131.1 (C-5^{Ph}), 123.4 (q, ¹*J*_{CF} = 274.0 Hz, CF₃), 123.4 (C-3^{Ph}), 119.7 (C-4^{Ph}), 118.8 (C-6^{Ph}), 56.2 (C-2^{Pip} and C-6^{Pip}), 29.1 (q, ²*J*_{CF} = 40.6 Hz, C^{diaziridine}), 25.1 (C-3^{Pip} and C-5^{Pip}), 23.0 (C-4^{Pip}) ppm. ¹⁹F NMR (282 MHz, methanol-*d*₄): δ –68.06 (s, CF₃) ppm. IR (ATR): $\bar{\nu}$ 3323, 3191, 1955, 1609, 1519, 1441, 1286, 1220, 1151, 1120, 1012, 872, 854, 723 cm⁻¹. HRMS (ESI-QTOF) *m/z*: calcd for C₁₃H₁₆F₃N₄⁺ [M + H]⁺, 285.1322; found, 285.1323.

5-Methyl-N-[2'-(piperidin-1-yl)-5'-[3-(trifluoromethyl)-3H-diaziridin-3-yl]phenyl]thiophene-2-sulfonamide (MK6–83^{PRG2}, 3b).

Note that this reaction was performed in the dark to avoid partial photolysis of the product (aluminum foil was used to cover flasks and columns). Under an argon atmosphere, 5-methylthiophene-2-sulfonyl chloride (610 mg, 3.10 mmol, 1.00 equiv) was added dropwise to a solution of **18b** (994 mg, 3.10 mmol, 1.00 equiv) in anhydrous pyridine (25 mL) at 0 °C. The mixture was stirred for 1 h at 0 °C and at room temperature overnight. The solvent was removed under reduced pressure and the residue dissolved in EtOAc (100 mL). The organic layer was washed with a NH₄Cl (aq) solution (saturated, 2 × 100 mL) and a solution of NaCl (aq) (saturated, 1 × 100 mL), dried over Na₂SO₄ and concentrated under reduced pressure. After purification by column chromatography on silica gel (⁴Hex/EtOAc = 30:1), the title compound was isolated as a light-yellow solid (991 mg, 2.23 mmol, 72% yield). In general, no further purification was required in this step. However, if necessary, preparative HPLC purification (C₁₈, eluent A, Milli-Q-grade water; eluent B, acetonitrile, isocratic (30:70) over 90 min with a flow rate of 12.5 mL min⁻¹ and detection at 254 nm) can be performed. *R*_f = 0.21 (SiO₂, ⁴Hex/EtOAc = 10:1). Mp: 107–109 °C. ¹H NMR, COSY (400 MHz, DMSO-*d*₆): δ 9.15 (s, 1H, NH), 7.39 (d, ³*J* = 3.8 Hz, 1H, *H*-3^{Thio}), 7.19 (d, ³*J* = 8.4 Hz, 1H, *H*-3^{Ph}), 7.19 (dd, ⁴*J* = 2.3, *J* = 0.8 Hz, 1H, *H*-6^{Ph}), 7.4 (dd, ³*J* = 8.4 Hz, ⁴*J* = 2.3 Hz, 1H, *H*-

$^4\text{P}^{\text{h}}$), 6.88 (dd, $^3J = 3.8$ Hz, $^4J = 1.4$ Hz, 1H, $H-4^{\text{Thio}}$), 2.66–2.59 (m, 4H, $2 \times H-2^{\text{Pip}}$ and $2 \times H-6^{\text{Pip}}$), 2.47 (d, $^4J = 1.1$ Hz, 3H, CH_3), 1.66–1.56 (m, 4H, $2 \times H-3^{\text{Pip}}$ and $2 \times H-5^{\text{Pip}}$), 1.52–1.42 (m, 2H, $2 \times H-4^{\text{Pip}}$) ppm. $^{13}\text{C}\{^1\text{H}\}$ NMR, HSQC, HMBC (100.6 MHz, $\text{DMSO}-d_6$): δ 148.0 ($C-2^{\text{Thio}}$), 147.1 ($C-2^{\text{Ph}}$), 137.0 ($C-5^{\text{Thio}}$), 132.9 ($C-3^{\text{Thio}}$), 131.8 ($C-1^{\text{Ph}}$), 126.3 ($C-4^{\text{Thio}}$), 123.5 ($C-4^{\text{Ph}}$), 122.4 ($C-5^{\text{Ph}}$), 122.1 ($C-3^{\text{Ph}}$), 121.8 (q, $^1J_{\text{CF}} = 274.9$ Hz, CF_3), 119.3 ($C-6^{\text{Ph}}$), 52.5 ($C-2^{\text{Pip}}$ and $C-6^{\text{Pip}}$), 27.8 (q, $^2J_{\text{CF}} = 39.9$ Hz, $\text{C}_q^{\text{diazirine}}$), 25.5 ($C-3^{\text{Pip}}$ and $C-5^{\text{Pip}}$), 23.5 ($C-4^{\text{Pip}}$), 15.1 (CH_3) ppm. ^{19}F NMR (376 MHz, $\text{DMSO}-d_6$): δ -65.81 (CF_3) ppm. IR (ATR): $\bar{\nu}$ 3245, 2947, 2811, 1515, 1436, 1337, 1228, 1144, 1021, 921, 906, 822, 806, 721 cm^{-1} . HRMS (ESI-QTOF) m/z : calcd for $\text{C}_{18}\text{H}_{20}\text{F}_3\text{N}_4\text{O}_2\text{S}_2^+ [\text{M} + \text{H}]^+$, 445.0974; found, 445.0974. HPLC analysis: retention time = 4.87 min; peak area = 99.60%; eluent A = Milli-Q-grade water; eluent B = CH_3CN ; eluent C = 0.1% solution of formic acid in Milli-Q-grade water; isocratic (20:70:10) over 8 min with a flow rate of 0.7 mL min^{-1} and detection at 254 nm; injection volume = 5 μL ; column temperature = 40 $^\circ\text{C}$.

PHOTOCHEMICAL KINETIC STUDIES AND INSTRUMENTATION

The photoactivation studies were performed according to procedures as reported by Brunner et al.³⁴ and Seifert et al.⁶⁰ using a high-power UV LED ($\lambda_{\text{max}} = 365$ nm; UV LED smart; Opsytec Dr. Gröbel GmbH) with the “standard” optic for a small spot diameter and a focused beam profile. Please refer to the homepage of the UV light source supplier (<https://www.opsytec.com/products/uv-led-light-sources>) for further details. Irradiation experiments were conducted within a ventilated fume hood in quartz cuvettes ($d = 10$ mm) including a tiny magnetic stirring bar placed 2 cm from the light source for very effective photoactivation. Under these conditions, no further cooling was necessary to maintain ambient temperature since the development of heat by the LED light source is negligible. A typical reaction setup is shown in Figure S9 (Supporting Information). For the analysis of the photolytic decay via ^{19}F NMR spectroscopy, (trifluoromethyl)diazirines **3a** and **3b** were dissolved in methanol- d_4 or cyclohexane- d_{12} ($c = 5$ mM), and after different irradiation intervals, samples were transferred and measured in 5 mm NMR amber glass tubes (type: S07-HP-AT-7 by Norell) before irradiation was continued. In HPLC-MS photolysis experiments, aliquots of 50 μL were collected from solutions of the diazirines **3a** and **3b** in selected solvents (HPLC-MS grade; $c = 2$ mm (methanol and cyclohexane) or $c = 50$ μM (aqueous buffer)), diluted (1:10 v/v) with acetonitrile/water (1:1 v/v), filtered through PTFE syringe filters ($d = 13$ mm, 0.2 μm pore size) and subsequently injected (injection volume = 5–10 μL) in the HPLC-MS system described above.

ASSOCIATED CONTENT

Supporting Information

The Supporting Information is available free of charge at <https://pubs.acs.org/doi/10.1021/acs.joc.0c02993>.

HPLC traces of key target compounds **3a** and **3b**, details about the crystal structures, the fragmentation pattern of diazirines **3a** and **3b**, ^{19}F NMR and LC-MS kinetic data of photolysis of compound **3b**, and ^1H and ^{13}C NMR spectra for all synthesized compounds (PDF)

Accession Codes

CCDC 2046164–2046165 contain the supplementary crystallographic data for this paper. These data can be obtained free of charge via www.ccdc.cam.ac.uk/data_request/cif, or by emailing data_request@ccdc.cam.ac.uk, or by contacting The Cam-

bridge Crystallographic Data Centre, 12 Union Road, Cambridge CB2 1EZ, UK; fax: +44 1223 336033.

AUTHOR INFORMATION

Corresponding Author

Tanja Schirmeister – Institute of Pharmaceutical and Biomedical Sciences, Johannes Gutenberg University Mainz, 55128 Mainz, Germany; Email: schirmei@uni-mainz.de

Authors

Kevin Schwickert – Institute of Pharmaceutical and Biomedical Sciences, Johannes Gutenberg University Mainz, 55128 Mainz, Germany; orcid.org/0000-0002-2575-0380

Michał Andrzejewski – Department of Chemistry, Biochemistry and Pharmaceutical Sciences, University of Bern, 3012 Bern, Switzerland

Simon Grabowsky – Department of Chemistry, Biochemistry and Pharmaceutical Sciences, University of Bern, 3012 Bern, Switzerland; orcid.org/0000-0002-3377-9474

Complete contact information is available at: <https://pubs.acs.org/10.1021/acs.joc.0c02993>

Notes

The authors declare no competing financial interest.

ACKNOWLEDGMENTS

We thank Dr. Johannes C. Liermann and Nadine Schenk (Department of Chemistry, Johannes Gutenberg University Mainz) for NMR spectroscopy, Dr. Christopher Kampf (Department of Chemistry, Johannes Gutenberg University Mainz) for high-resolution mass spectrometry, and Mergim Meta and Tobias Ott for assisting with syntheses.

REFERENCES

- (1) Sun, M.; Goldin, E.; Stahl, S.; Falardeau, J. L.; Kennedy, J. C.; Acierno, J. S., Jr; Bove, C.; Kaneski, C. R.; Nagle, J.; Bromley, M. C.; Colman, M.; Schiffmann, R.; Slausenhaupt, S. A. Mucopolipidosis type IV is caused by mutations in a gene encoding a novel transient receptor potential channel. *Hum. Mol. Genet.* **2000**, *9*, 2471–2478.
- (2) Bach, G. Mucopolipidosis Type IV. *Mol. Genet. Metab.* **2001**, *73*, 197–203.
- (3) Wakabayashi, K.; Gustafson, A. M.; Sidransky, E.; Goldin, E. Mucopolipidosis type IV: An update. *Mol. Genet. Metab.* **2011**, *104*, 206–213.
- (4) Smith, J. A.; Chan, C.-C.; Goldin, E.; Schiffmann, R. Noninvasive diagnosis and ophthalmic features of mucopolipidosis type IV. *Ophthalmology* **2002**, *109*, 588–594.
- (5) Schiffmann, R.; Dwyer, N. K.; Lubensky, I. A.; Tsokos, M.; Sutliff, V. E.; Latimer, J. S.; Frei, K. P.; Brady, R. O.; Barton, N. W.; Blanchette-Mackie, E. J.; Goldin, E. Constitutive achlorhydria in mucopolipidosis type IV. *Proc. Natl. Acad. Sci. U. S. A.* **1998**, *95*, 1207–1212.
- (6) Altarescu, G.; Sun, M.; Moore, D. F.; Smith, J. A.; Wiggs, E. A.; Solomon, B. I.; Patronas, N. J.; Frei, K. P.; Gupta, S.; Kaneski, C. R.; Quarrell, O. W.; Slausenhaupt, S. A.; Goldin, E.; Schiffmann, R. The neurogenetics of mucopolipidosis type IV. *Neurology* **2002**, *59*, 306–313.
- (7) Berman, E. R.; Livni, N.; Shapira, E.; Merin, S.; Levij, I. S. Congenital corneal clouding with abnormal systemic storage bodies: A new variant of mucopolipidosis. *J. Pediatr.* **1974**, *84*, 519–526.
- (8) Merin, S.; Livni, N.; Berman, E. R.; Yatziv, S. Mucopolipidosis IV: ocular, systemic, and ultrastructural findings. *Investigative Ophthalmology & Visual Science* **1975**, *14*, 437–448.
- (9) Zeevi, D. A.; Frumkin, A.; Bach, G. TRPML and lysosomal function. *Biochim. Biophys. Acta, Mol. Basis Dis.* **2007**, *1772*, 851–858.
- (10) Bargal, R.; Avidan, N.; Ben-Asher, E.; Olender, Z.; Zeigler, M.; Frumkin, A.; Raas-Rothschild, A.; Glusman, G.; Lancet, D.; Bach, G.

Identification of the gene causing mucopolipidosis type IV. *Nat. Genet.* **2000**, *26*, 118–122.

(11) Bassi, M. T.; Manzoni, M.; Monti, E.; Pizzo, M. T.; Ballabio, A.; Borsani, G. Cloning of the Gene Encoding a Novel Integral Membrane Protein, Mucopolipidin—and Identification of the Two Major Founder Mutations Causing Mucopolipidosis Type IV. *Am. J. Hum. Genet.* **2000**, *67*, 1110–1120.

(12) Venkatachalam, K.; Montell, C. TRP Channels. *Annu. Rev. Biochem.* **2007**, *76*, 387–417.

(13) Li, M.; Zhang, W. K.; Benveniste, N. M.; Zhou, X.; Su, D.; Li, H.; Wang, S.; Michailidis, I. E.; Tong, L.; Li, X.; Yang, J. Structural basis of dual Ca²⁺/pH regulation of the endolysosomal TRPML1 channel. *Nat. Struct. Mol. Biol.* **2017**, *24*, 205–213.

(14) Cheng, X.; Shen, D.; Samie, M.; Xu, H. Mucopolipins: Intracellular TRPML1–3 channels. *FEBS Lett.* **2010**, *584*, 2013–2021.

(15) Viet, K. K.; Wagner, A.; Schwickert, K.; Hellwig, N.; Brennich, M.; Bader, N.; Schirmeister, T.; Morgner, N.; Schindelin, H.; Hellmich, U. A. Structure of the Human TRPML2 Ion Channel Extracytosolic/Luminal Domain. *Structure* **2019**, *27*, 1246–1257.e5.

(16) Venkatachalam, K.; Wong, C.-O.; Zhu, M. X. The role of TRPMLs in endolysosomal trafficking and function. *Cell Calcium* **2015**, *58*, 48–56.

(17) Chen, C.-C.; Keller, M.; Hess, M.; Schiffmann, R.; Urban, N.; Wolfgang, A.; Schaefer, M.; Bracher, F.; Biel, M.; Wahl-Schott, C.; Grimm, C. A small molecule restores function to TRPML1 mutant isoforms responsible for mucopolipidosis type IV. *Nat. Commun.* **2014**, *5*, 4681.

(18) Grimm, C.; Jörs, S.; Saldanha, S. A.; Obukhov, A. G.; Pan, B.; Oshima, K.; Cuajungco, M. P.; Chase, P.; Hodder, P.; Heller, S. Small Molecule Activators of TRPML3. *Chem. Biol.* **2010**, *17*, 135–148.

(19) Shen, D.; Wang, X.; Li, X.; Zhang, X.; Yao, Z.; Dibble, S.; Dong, X.-p.; Yu, T.; Lieberman, A. P.; Showalter, H. D.; Xu, H. Lipid storage disorders block lysosomal trafficking by inhibiting a TRP channel and lysosomal calcium release. *Nat. Commun.* **2012**, *3*, 731.

(20) Schmiede, P.; Fine, M.; Blobel, G.; Li, X. Human TRPML1 channel structures in open and closed conformations. *Nature* **2017**, *550*, 366–370.

(21) Zhou, X.; Li, M.; Su, D.; Jia, Q.; Li, H.; Li, X.; Yang, J. Cryo-EM structures of the human endolysosomal TRPML3 channel in three distinct states. *Nat. Struct. Mol. Biol.* **2017**, *24*, 1146–1154.

(22) Grimm, C. Endolysosomal Cation Channels as Therapeutic Targets—Pharmacology of TRPML Channels. *Messenger* **2016**, *5*, 30–36.

(23) Leis, S.; Schneider, S.; Zacharias, M. In Silico Prediction of Binding Sites on Proteins. *Curr. Med. Chem.* **2010**, *17*, 1550–1562.

(24) Ludington, J. L. In *Fragment-Based Methods in Drug Discovery*; Klon, A. E., Ed.; Springer New York: New York, NY, 2015; pp 145–154.

(25) Robinette, D.; Neamati, N.; Tomer, K. B.; Borchers, C. H. Photoaffinity labeling combined with mass spectrometric approaches as a tool for structural proteomics. *Expert Rev. Proteomics* **2006**, *3*, 399–408.

(26) Smith, E.; Collins, I. Photoaffinity labeling in target- and binding-site identification. *Future Med. Chem.* **2015**, *7*, 159–183.

(27) Hashimoto, M.; Hatanaka, Y. Recent Progress in Diazirine-Based Photoaffinity Labeling. *Eur. J. Org. Chem.* **2008**, *2008*, 2513–2523.

(28) Hatanaka, Y. Development and Leading-Edge Application of Innovative Photoaffinity Labeling. *Chem. Pharm. Bull.* **2015**, *63*, 1–12.

(29) Sadakane, Y.; Hatanaka, Y. Photochemical Fishing Approaches for Identifying Target Proteins and Elucidating the Structure of a Ligand-binding Region Using Carbene-generating Photoreactive Probes. *Anal. Sci.* **2006**, *22*, 209–218.

(30) Dormán, G.; Prestwich, G. D. Using photolabile ligands in drug discovery and development. *Trends Biotechnol.* **2000**, *18*, 64–77.

(31) Brunner, J. New Photolabeling and Crosslinking Methods. *Annu. Rev. Biochem.* **1993**, *62*, 483–514.

(32) Dubinsky, L.; Krom, B. P.; Meijler, M. M. Diazirine based photoaffinity labeling. *Bioorg. Med. Chem.* **2012**, *20*, 554–570.

(33) Lapinsky, D. J. Tandem photoaffinity labeling—bioorthogonal conjugation in medicinal chemistry. *Bioorg. Med. Chem.* **2012**, *20*, 6237–6247.

(34) Brunner, J.; Senn, H.; Richards, F. M. 3-Trifluoromethyl-3-phenyldiazirine. A new carbene generating group for photolabeling reagents. *J. Biol. Chem.* **1980**, *255*, 3313–3318.

(35) Hill, J. R.; Robertson, A. A. B. Fishing for Drug Targets: A Focus on Diazirine Photoaffinity Probe Synthesis. *J. Med. Chem.* **2018**, *61*, 6945.

(36) Kwong, F. Y.; Klapars, A.; Buchwald, S. L. Copper-Catalyzed Coupling of Alkylamines and Aryl Iodides: An Efficient System Even in an Air Atmosphere. *Org. Lett.* **2002**, *4*, 581–584.

(37) Old, D. W.; Wolfe, J. P.; Buchwald, S. L. A Highly Active Catalyst for Palladium-Catalyzed Cross-Coupling Reactions: Room-Temperature Suzuki Couplings and Amination of Unactivated Aryl Chlorides. *J. Am. Chem. Soc.* **1998**, *120*, 9722–9723.

(38) Driver, M. S.; Hartwig, J. F. A Second-Generation Catalyst for Aryl Halide Amination: Mixed Secondary Amines from Aryl Halides and Primary Amines Catalyzed by (DPPF)PdCl₂. *J. Am. Chem. Soc.* **1996**, *118*, 7217–7218.

(39) Fujita, K.-i.; Takahashi, Y.; Owaki, M.; Yamamoto, K.; Yamaguchi, R. Synthesis of Five-, Six-, and Seven-Membered Ring Lactams by Cp*Rh Complex-Catalyzed Oxidative N-Heterocyclization of Amino Alcohols. *Org. Lett.* **2004**, *6*, 2785–2788.

(40) Kotha, S.; Shah, V. R. Design and Synthesis of 1-Benzazepine Derivatives by Strategic Utilization of Suzuki–Miyaura Cross-Coupling, Aza-Claisen Rearrangement and Ring-Closing Metathesis. *Eur. J. Org. Chem.* **2008**, *2008*, 1054–1064.

(41) Yin, Y.; Cameron, M. D.; Lin, L.; Khan, S.; Schröter, T.; Grant, W.; Pocas, J.; Chen, Y. T.; Schürer, S.; Pachori, A.; LoGrasso, P.; Feng, Y. Discovery of Potent and Selective Urea-Based ROCK Inhibitors and Their Effects on Intraocular Pressure in Rats. *ACS Med. Chem. Lett.* **2010**, *1*, 175–179.

(42) Bartoli, G.; Bosco, M.; Locatelli, M.; Marcantoni, E.; Massaccesi, M.; Melchiorre, P.; Sambri, L. A Lewis Acid-Mediated Protocol for the Protection of Aryl Amines as their Boc-Derivatives. *Synlett* **2004**, *2004*, 1794–1798.

(43) Kelly, T. A.; McNeil, D. W. A simple method for the protection of aryl amines as their t-butylcarbonyl (Boc) derivatives. *Tetrahedron Lett.* **1994**, *35*, 9003–9006.

(44) Moyer, M. P.; Shiurba, J. F.; Rapoport, H. Metal-halogen exchange of bromoindoles. A route to substituted indoles. *J. Org. Chem.* **1986**, *51*, 5106–5110.

(45) DiMenna, W. S. A convenient preparation of aryltrifluoromethylketones. *Tetrahedron Lett.* **1980**, *21*, 2129–2132.

(46) Nahm, S.; Weinreb, S. M. N-methoxy-n-methylamides as effective acylating agents. *Tetrahedron Lett.* **1981**, *22*, 3815–3818.

(47) Trabbic, C. J.; Overmeyer, J. H.; Alexander, E. M.; Crissman, E. J.; Kvale, H. M.; Smith, M. A.; Erhardt, P. W.; Maltese, W. A. Synthesis and Biological Evaluation of Indolyl-Pyridinyl-Propenones Having Either Methuosis or Microtubule Disruption Activity. *J. Med. Chem.* **2015**, *58*, 2489–2512.

(48) Dolomanov, O. V.; Bourhis, L. J.; Gildea, R. J.; Howard, J. A. K.; Puschmann, H. OLEX2: a complete structure solution, refinement and analysis program. *J. Appl. Crystallogr.* **2009**, *42*, 339–341.

(49) Sheldrick, G. SHELXT - Integrated space-group and crystal-structure determination. *Acta Crystallogr., Sect. A: Found. Adv.* **2015**, *71*, 3–8.

(50) Sheldrick, G. Crystal structure refinement with SHELXL. *Acta Crystallogr., Sect. C: Struct. Chem.* **2015**, *71*, 3–8.

(51) Grabowsky, S.; Luger, P.; Buschmann, J.; Schneider, T.; Schirmeister, T.; Sobolev, A. N.; Jayatilaka, D. The Significance of Ionic Bonding in Sulfur Dioxide: Bond Orders from X-ray Diffraction Data. *Angew. Chem., Int. Ed.* **2012**, *51*, 6776–6779.

(52) Schneider, T. H.; Rieger, M.; Ansorg, K.; Sobolev, A. N.; Schirmeister, T.; Engels, B.; Grabowsky, S. Vinyl sulfone building blocks in covalently reversible reactions with thiols. *New J. Chem.* **2015**, *39*, 5841–5853.

- (53) Grabowsky, S.; Pfeuffer, T.; Chęcińska, L.; Weber, M.; Morgenroth, W.; Luger, P.; Schirmeister, T. Electron-Density Determination of Electrophilic Building Blocks as Model Compounds for Protease Inhibitors. *Eur. J. Org. Chem.* **2007**, *2007*, 2759–2768.
- (54) Grabowsky, S.; Pfeuffer, T.; Morgenroth, W.; Paulmann, C.; Schirmeister, T.; Luger, P. A comparative study on the experimentally derived electron densities of three protease inhibitor model compounds. *Org. Biomol. Chem.* **2008**, *6*, 2295–2307.
- (55) Mladenovic, M.; Arnone, M.; Fink, R. F.; Engels, B. Environmental Effects on Charge Densities of Biologically Active Molecules: Do Molecule Crystal Environments Indeed Approximate Protein Surroundings? *J. Phys. Chem. B* **2009**, *113*, 5072–5082.
- (56) Kleemiss, F.; Wieduwilt, E. K.; Hupf, E.; Shi, M. W.; Stewart, S. G.; Jayatilaka, D.; Turner, M. J.; Sugimoto, K.; Nishibori, E.; Schirmeister, T.; Schmidt, T. C.; Engels, B.; Grabowsky, S. Similarities and Differences between Crystal and Enzyme Environmental Effects on the Electron Density of Drug Molecules. *Chem. - Eur. J.* **2021**, *27*, 3407–3419.
- (57) Spackman, M. A.; Jayatilaka, D. Hirshfeld surface analysis. *CrystEngComm* **2009**, *11*, 19–32.
- (58) Brammer, L. Halogen bonding, chalcogen bonding, pnictogen bonding, tetrel bonding: origins, current status and discussion. *Faraday Discuss.* **2017**, *203*, 485–507.
- (59) Turner, M. J.; Wolff, S. K.; Grimwood, D. J.; Spackman, P. R.; Jayatilaka, D.; Spackman, M. A. University of Western Australia, 2017.
- (60) Seifert, T.; Malo, M.; Lengqvist, J.; Sihlbom, C.; Jarho, E. M.; Luthman, K. Identification of the Binding Site of Chroman-4-one-Based Sirtuin 2-Selective Inhibitors using Photoaffinity Labeling in Combination with Tandem Mass Spectrometry. *J. Med. Chem.* **2016**, *59*, 10794–10799.
- (61) Babu Kumar, A.; Anderson, J. M.; Manetsch, R. Design, synthesis and photoactivation studies of fluorinated photolabels. *Org. Biomol. Chem.* **2011**, *9*, 6284–6292.
- (62) Kumar, A. B.; Tipton, J. D.; Manetsch, R. 3-Trifluoromethyl-3-aryldiazirine photolabels with enhanced ambient light stability. *Chem. Commun.* **2016**, *52*, 2729–2732.
- (63) Wang, J.; Kubicki, J.; Gustafson, T. L.; Platz, M. S. The Dynamics of Carbene Solvation: An Ultrafast Study of p-Biphenyltrifluoromethylcarbene. *J. Am. Chem. Soc.* **2008**, *130*, 2304–2313.
- (64) Wang, J.; Kubicki, J.; Peng, H.; Platz, M. S. Influence of Solvent on Carbene Intersystem Crossing Rates. *J. Am. Chem. Soc.* **2008**, *130*, 6604–6609.
- (65) Creary, X. Regioselectivity in the addition of singlet and triplet carbenes to 1,1-dimethylallene. A probe for carbene multiplicity. *J. Am. Chem. Soc.* **1980**, *102*, 1611–1618.
- (66) Mueller, P. H.; Rondan, N. G.; Houk, K. N.; Harrison, J. F.; Hooper, D.; Willen, B. H.; Liebman, J. F. Carbene singlet-triplet gaps. Linear correlations with substituent pi-donation. *J. Am. Chem. Soc.* **1981**, *103*, 5049–5052.
- (67) Moss, R. A.; Perez, L. A.; Turro, N. J.; Gould, I. R.; Hacker, N. P. Hammett analysis of absolute carbene addition rate constants. *Tetrahedron Lett.* **1983**, *24*, 685–688.
- (68) Griller, D.; Liu, M. T. H.; Scaiano, J. C. Hydrogen bonding in alcohols: its effect on the carbene insertion reaction. *J. Am. Chem. Soc.* **1982**, *104*, 5549–5551.
- (69) Das, J. Aliphatic Diazirines as Photoaffinity Probes for Proteins: Recent Developments. *Chem. Rev.* **2011**, *111*, 4405–4417.
- (70) Platz, M.; Admasu, A. S.; Kwiatkowski, S.; Crocker, P. J.; Imai, N.; Watt, D. S. Photolysis of 3-aryl-3-(trifluoromethyl)diazirines: a caveat regarding their use in photoaffinity probes. *Bioconjugate Chem.* **1991**, *2*, 337–341.
- (71) Wrasidlo, W. J.; Stocking, E. M.; Price, D. L.; Natala, S. R., Substituted Phenyl Sulfonyl Phenyl Triazole Thiones and Uses Thereof, Neuropeptide Therapies, I., 2019, Patent WO2019/089478A1.
- (72) Overlapping signals.
- (73) Li, J.; Wu, F.; Liu, X.; Zou, Y.; Chen, H.; Li, Z.; Zhang, L. Synthesis and bioevaluation of 1-phenyl-pyrazole-4-carboxylic acid derivatives as potent xanthine oxidoreductase inhibitors. *Eur. J. Med. Chem.* **2017**, *140*, 20–30.
- (74) Overlapping signals.